ASTRONOMY & ASTROPHYSICS
SUPPLEMENT SERIES

NOVEMBER II **1996**, PAGE 157

Astron. Astrophys. Suppl. Ser. **120,** 157-177 (1996)

The β Pictoris phenomenon among Herbig Ae/Be stars.

UV and optical high dispersion spectra*

C.A. Grady[1,2], M.R. Pérez[2], A. Talavera[3], K.S. Bjorkman[4], D. de Winter[5], P.-S. Thé[5], F.J. Molster[5], M.E. van den Ancker[5], M.L. Sitko[6], N.D. Morrison[7], M.L. Beaver[7,8], B. McCollum[9] and M.W. Castelaz[10]

[1] Eureka Scientific, 2452 Delmer Street, Suite 100, Oakland CA 94602, U.S.A.
[2] Applied Research Corp., Suite 1120, 8201 Corporate Dr., Landover, MD 20785, U.S.A.
[3] Laboratorio de Astrofisica Espacial y Fisica Fundamental, I.N.T.A., Apartado 50727, 28080- Madrid, Spain
[4] Space Astronomy Laboratory, University of Wisconsin, Madison WI 53706-1390, U.S.A.
[5] Astronomical Institute "Anton Pannekoek", University of Amsterdam, Kruislaan 403, 1098 SJ Amsterdam, The Netherlands
[6] Department of Physics, University of Cincinnati, Cincinnati OH 45221-0011, U.S.A.
[7] Ritter Observatory and Department of Physics and Astronomy, University of Toledo, Toledo OH 43606, U.S.A.
[8] Department of Physics and Astronomy, Michigan State University, East Lansing, MI 48824, U.S.A.
[9] CSC-IUE Observatory, GSFC, Greenbelt, MD 20771, U.S.A.
[10] Department of Physics, East Tennessee State University, Box 70652, Johnson City TN 37614, U.S.A.

Received August 30, 1995; accepted April 10, 1996

Abstract. — We present a survey of high dispersion UV and optical spectra of Herbig Ae/Be (HAeBe) and related stars. We find accreting, circumstellar gas over the velocity range +100 to +400 km s^{-1}, and absorption profiles similar to those seen toward β Pic, in 36% of the 33 HAeBe stars with IUE data as well as in 3 non-emission B stars. We also find evidence of accretion in 7 HAeBe stars with optical data only. Line profile variability appears ubiquitous. As a group, the stars with accreting gas signatures have higher $v \sin i$ than the stars with outflowing material, and tend to exhibit large amplitude ($\geq 1^m$) optical light variations. All of the program stars with polarimetric variations that are anti-correlated with the optical light, previously interpreted as the signature of a dust disk viewed close to equator-on, also show spectral signatures of accreting gas. These data imply that accretion activity in HAeBe stars is preferentially observed when the line of sight transits the circumstellar dust disk. Our data imply that the spectroscopic signatures of accreting circumstellar material seen in β Pic are not unique to that object, but instead are consistent with interpretation of β Pic as a comparatively young A star with its associated circumstellar disk.

Key words: stars: β Pic: pre-main sequence — circumstellar matter — line: profiles — ultraviolet: stars

1. Introduction

After a decade of intense study, one of the more intriguing questions posed by β Pictoris is how frequently and under what circumstances do large circumstellar dust disks like that surrounding β Pic result as a remnant or byproduct of star formation. Surveys of field A stars have demonstrated that IR excesses consistent with material at or beyond Kuiper belt distances are common around Main Sequence stars, whereas multi-temperature IR excesses, consistent with the presence of small dust grains both distant from, and comparatively close to the star, are much less common (Aumann 1985; Oudmaijer et al. 1992; Stencel & Backman 1991). Accreting gas has also been detected in the line of sight to a few other A and late B stars (Lagrange-Henri et al. 1990; Grady et al. 1991), but has not been observed toward the majority of field A stars with circumstellar dust. This suggests that either dust and gas disks like β Pic are rare around Main Sequence stars, or that they represent a short-lived evolutionary phase. If the presence of such a dust disk is a short-lived evolutionary phase, occurring near the end of the pre-Main Sequence (PMS) lifetime of the star, similar disks together with spectroscopic signatures of accreting material should be detectable around

Send offprint requests to: C.A. Grady via e-mail at cgrady@mtolympus.ari.net

*Based on observations made with the *International Ultraviolet Explorer* operated by NASA and ESA, and at the European Southern Observatory, La Silla, Chile, the Cerro Tololo Inter-American Observatory of the National Optical Astronomy Observatories, and the Ritter Observatory of the University of Toledo

the evolutionary precursors of β Pic, the Herbig Ae and related stars.

2. Observations and archival spectral data

Over the past 18 years, the *International Ultraviolet Explorer* has obtained an extensive database of mid and far UV spectra of Herbig Ae/Be (HAeBe) stars covering 1150−3200 Å for some 64 stars. A table listing the stars with observations current as of late 1993 is given in Talavera & Verdugo (1994). In addition to low dispersion spectra, the IUE archives contain high dispersion spectra with a resolution of 25 km s^{-1} of some 36 stars from the catalog of Thé et al. (1994) and the IR-selected sample from Bogaert et al. (1995). The IUE high dispersion spectra are biased toward HAeBe stars which are bright in the UV, or which are known large amplitude photometric variables. However, due to scheduling limitations and oversubscription on the Hubble Space Telescope, the IUE data are likely to remain the most comprehensive UV spectral dataset with a resolution sufficient to identify outflowing or accreting circumstellar material for the foreseeable future. The IUE data are unique in another regard: the long mission duration has made multiple observations feasible, permitting sporadic monitoring of a number of the brighter objects. These spectra have been supplemented with optical spectra obtained from 1993-1995 with the Coudé Auxilliary Telescope of the European Southern Observatory, the 1-m telescope of the Ritter Observatory, and the 1-m at Cerro Tololo Inter-American Observatory.

2.1. *UV spectra of Herbig Ae/Be stars*

Due to the stability of the IUE cameras, the data have been uniformly reduced, as described in Pérez et al. (1993a). Wavelength coverage is most complete for the UV-luminous Herbig Be stars which typically have both far UV (FUV) (1150−2000 Å) and mid-UV (2000−3200 Å) high dispersion IUE spectra. Due to the camera sensitivity as a function of wavelength, the mid-UV spectra are well-exposed only from 2500−3200 Å. The Herbig Ae (HAe) stars in our sample are typically represented by mid-UV data only. Due to the 3 magnitude range in brightness of our program stars, together with the limited dynamic range of the IUE detectors, the S/N of the high dispersion spectra ranges from levels consistent with optimally exposed data (S/N=13−15 near 2800 Å for the brightest program stars and up to 11.5 near C IV for the early type B stars) down to S/N=3−6 near Mg II for the fainter HAe stars. Velocities, unless noted, are given in the IUE reference system. Errors of up to 8−10 km s^{-1} relative to true heliocentric velocities have been noted for the LWR/P data (Boggess et al. 1991). The program stars are listed in Tables 1 and 2.

2.2. *The optical spectra*

Optical spectra of a number of southern HAeBe stars which are known or suspected large amplitude photometric variables from the catalog of Thé et al. (1994) were obtained in July 1993, October 1993, and January 1995 in the vicinity of Hα and the Na I D lines with the Coudé Auxiliary Telescope (CAT) at La Silla. The short camera was used, equipped with an RCA high resolution CCD of 1024 × 640, 15 × 15 μm, pixels, without any binning. Details of each observation, together with a discussion of the individual stars are given in Appendix A and Table 4. The wavelength ranges are 6535−6590 Å for the Hα and 5860−5910 Å for the Na I D regions. The spectra were reduced at ESO headquarters using the MIDAS software running under Sun/OS. The spectra were optimally extracted using the algorithm of Horne (1986). With the resolution of 50 000 for the Hα and 55 000 for the Na I D region our set-up resulted in a final resolving power, after rebinning to heliocentric velocity, of 2.54 and 2.58 km s^{-1} pixel^{-1}, respectively. Under good weather condictions a S/N of 50 was reached for a star with $V \sim 9^{\rm m}$.

Additional optical spectra of some of the brighter variable HAeBe stars were obtained with a fiber-fed échelle spectrograph attached to the 1-m telescope of the Ritter Observatory and to a Wright Instruments Ltd. CCD camera, incorporating a 800 × 1200 EEV CCD with pixel dimensions of 22.5 × 22.5 μm. With the spectrograph in high throughput mode, one spectral resolution element corresponds to ≈4 pixels FWHM and $R \simeq 26000$. In good sky conditions, a 60 minute exposure yielded a continuum $S/N\sim$ 100 for $V \simeq 7$. The spectral coverage consistes of 9 disjoint 70 Å regions in the yellow and red, including Hα, the Na I D lines, He Iλ5876, and Si II$\lambda\lambda$ 6347, 6371 (not shown here). The data were reduced with IRAF version 2.10.3β.

3. The spectra

Previous UV studies of HAeBe stars have either focussed on Mg II or have intensively monitored individual objects. Imhoff (1994) noted a wide variety of Mg II emission profile types for the HAeBe stars, including Beals (1950) type I P Cygni profiles with shortward-shifted absorption indicative of the presence of strong stellar winds, stars with interstellar-like Mg II absorption, and double emission profiles (Beals type III) including, in some cases, longward-shifted absorption indicative of the presence of accreting gas. We will first summarize the data for the HAeBe stars with spectral signatures of the presence of strong stellar winds and those stars with IS-like features only, and then discuss the stars with spectral signatures of accreting gas in both the HAeBe stars and in some non-emission line, but plausibly young A and B stars. The stars with wind detections or IS-like spectra are listed in

Table 1. HAeBe stars with outflow signatures, veiled spectra, or interstellar-like absorption features only. The first column gives the stellar name or HD number. The second column gives the spectral type from Thé et al. (1994). The third column indicates the amplitude of photometric variation in magnitudes from Schevchenko et al. (1994), Thé et al. (1994) or the SIMBAD database. The fourth column indicates the presence of polarimetric variability of more than 1%. The fifth column shows the maximum wind outflow velocity in km s^{-1} with an average uncertainty of 25 km s^{-1}. The sixth column indicates the ion measured, and the seventh column lists the source of the wind detection. The eighth column indicates the overall appearance of Mg II, the ninth column gives the Hα data. I indicates a Beals (1951) type I P Cygni profile, whereas III indicates a double-peaked emission profile (Beals type III). IS indicates the presence of narrow absorption features similar to interstellar absorption, and e indicates the presence of emission, with no further information on the profile type. abs indicates the presence of blueshifted absorption with no emission component. The 10th column lists the IR excess in magnitudes; FF indicates an IR excess consistent with free-free emission rather than the presence of dust. The 11th column gives v sin i with the reference for the measurement in the 12th column. Uncertain data are indicated by: 1) Grady et al. 1988, 2) Imhoff 1994, 3) this study, 4) Talavera et al. 1982, 5) Catala et al. 1989, 6) Sonneborn et al. 1988, 7) Finkenzeller & Mundt 1984, 8) Hamann & Persson 1992, 9) Oudmaijer et al. 1992, 10) Hillenbrand et al. 1992, 11) Hillenbrand et al. 1995, 12) Finkenzeller 1985; 13) Slettebak 1982, 14) Böhm & Catala 1994, 15) Davis et al. 1983

Star Name	Spectral	Variability		Stellar Winds			Emission		12 μm	V sin i	Notes
	Type	Phot.	Pol.	Vel.	Ion	Ref.	Mg II.	Hα	Excess	km s^{-1}	
Stars with Winds											
HD 200775	B2e	0.08	N	-600	C IV	1	I	III	5.58	40	14,11
BD +65° 1637	B2/3e	0.23	N	-90	Mg II	2	IS	III	...	180	12, 10
HD 216629	B2/3	0.08	N		Mg II	2	IS	I	4.52	180	7,9
HD 87643	B3/4[e]	0.37	N	-700	Mg II	2	I	III	8.41	...	9
HD 259431	B5e	0.23	N	-400	C IV	1	I	III	6.61	40	11, 9
V380 Ori	B8-A1e	0.7	N	-1100	Mg II	2	I	S	6.98	20:	11, 10
HD 98922	B9 Ve	0.11	N	-300	Si II	3	I	I	6.33	...	9,
HD 179218	B9	0.5	N	-200	Mg II	3	abs	...	5.24	...	9
HD 250550	B9/A0	0.15	N	-600	MgII	4	I	I	6.53	70	11
AB Aur	A0e	1.2	N	-360v	MgII	4	I	I	6.23	100	7,11
HD 150193	A0-4e	0.22	N	-190	Mg II	2	I	I	6.14	100	12
HD 190073	A0IVesh	0.04	N	-400-600	Mg II	2	I		5.62		9
HD 163296	A1-2IIIe	0.19	N	-380v	MgII	5	I/III	I	5.67	120	12,10
HD 31648	A2e		N	-250	Mg II	2	I	III	5.21	...	9
HD 104237	A4e	...	...	-200	Mg II	2	I	III	5.27	...	9
BD +46° 3471	A4e	0.07	N	-300	Si II	4	I	I	7.30	100	11
Normal B Stars and Veiled UV Spectra:											
ω Ori	B2IIIe	0.18	Y	-800	C IV	6	IS	III	FF	160	13,10
HD 53367	B0e	0.04	N	-600:	C IV	3	IS	I	FF	30	14,10
HD 52721	B2Vnne	0.15	N	...	...	3	IS	I	FF	400	15,10
HD 76534	B2/3ne	0.11	N	...	...	2	IS	III	FF	110	12, 10
HD 97048	B9e	0.17	...	...	...	2	IS	I	5.89	140	14,10

Table 1. The stars with accretion signatures are listed in Table 2.

3.1. *Stars with spectral signatures of stellar winds*

In the ultraviolet, the presence of stellar or disk winds manifests as either Beals type I P Cygni profiles characterized by absorption shortward of line center and emission at longer wavelengths, or simply by shorward asymmetric absorption in the transitions of interest. In both cases the short wavelength edge of the absorption profile provides an estimate of the maximum outflow velocity. Sixteen of the 33 HAeBe stars with IUE high dispersion spectra have UV spectral signatures of outflowing material in Mg II and, where available, in other ions (Table 1). Several of these, including AB Aur, HD 259431, HD 200775, and V380 Ori are shown in Imhoff (1994). Outflow velocities of several hundred km s^{-1} are seen in all of these stars except BD +65° 1637, which shows lower velocity outflows in Mg II only. The presence of strong, high velocity stellar winds is atypical not only of normal stars in the spectral type range of these stars, but is also not seen in classical Be stars of similar spectral type and low v sin i (Grady et al. 1987, 1989). The program HAeBe stars differ from Main Sequence A and B stars also in the presence of shortward-shifted absorption in transitions to high-lying metastable levels of Fe II and other species, indicating the presence of high density gas in the wind. Previous studies of AB Aur (Praderie et al. 1986) have demonstrated that periodic modulation of the outflowing material occurs, and has been interpreted as occuring on the same time frame as the stellar rotation period. In the case of HD 163296 (Catala et al. 1991), outflow episodes lacking sustained periodicity have been detected. However, detection of outflowing material in only 48% of the program stars indicates that wind signatures, while common, are not ubiquitous among the HAeBe stars.

Table 2. HAeBe and related stars with accreting gas. Column 4 indicates the presence of polarimetric variability of $\geq$1%. Columns 5-7 show the maximum accretion velocity ($\pm$25 km s^{-1}), the ion measured, and the source of the detection. Columns 8-10 give the line profile types, with IP indicating inverse P Cygni, I* narrow emission with superposed IS absorption, and the other profile types as in Table 1. Column 11 gives the IR excess in magnitudes; C indicates a confused region. Columns 12 gives v sin i. References: 1) Sitko et al. 1994, 2) van den Ancker et al. 1995, 3) Schulte-Ladbeck et al. 1992, 4) Grinin et al. 1991, 5) Hutchinson et al. 1994, 6) Bjorkman et al. 1994, 7) Khardopolov et al. 1991, 8) Schevchenko et al. 1993, 9) Grady et al. 1993a, 10) Hutsemékers 1985, 11) this study, 12) Imhoff 1994, 13) Pérez et al. 1993a, 14) Graham 1992, 15) Grinin et al. 1995, 16) Welty et al. 1992, 17) Hamann & Persson 1992, 18) Ghandour et al. 1994, 19) Grady et al. 1993b, 22) Vidal-Madjar et al. 1994, 23) Böhm & Catala 1994, 24) Hillenbrand et al. 1995, 25) Slettebak 1982, 26) SIMBAD, 27) Davis et al. 1983, 28) Lecavelier des Etangs et al. 1995, 29) Bibo & Thé 1991, 30) van den Ancker et al. 1995a

Star Name	Sp.T.	Variable			Accretion			Emission			12μm	v sin i	Ref.
		Phot.	Pol.	Ref.	Max.	Ion	Ref.	Hα	Mg II	C IV			
HAeBe Stars with UV Detections:													
HD 45677	B2[e]	1.25	Y	1,2,3	+400	C IV	9	III	I*	abs	8.79	$\geq$200:	11
HD 37806	B8e	0.09	...	29	+400	C IV	11	III	I*	IP:	6.58	120	26
HD 37411	B9e	0.09:	...	26	+150	Mg II	12	III	abs	...	5.01	...	...
HD 58647	B9e	0.04:	...	26	+250	C IV	11	III	IP	IP	4.34	280:	11
UX Ori	A1-3IIIe	2.6	Y	4,8,29	+200	Mg II	11	III/IP	III	...	5.13	175	23
HD 95881	A2e	0.6	...	11	+300	C IV	11	III	III	abs	6.07	150:	11
HD 35187	A2e	...	...	...	+150	Mg II	11	III	abs	...	4.77	150:	11
HR 5999	A5e	1.7	Y	5,13,29	+250	Mg II	13	III	III/IP	e	5.13	135	23
HD 35929	A8e	...	...	...	+100	Zn II	11	I	III	e	3.23	150:	1
HAeBe Stars with Optical Detections:													
R CrA	B8e	3.6	Y	8,26	+500	Na I	14	III	e	...	10:	...	...
WW Vul	A1e	2.3	Y	4,8	+75	Na I	15	III	e	...	...	...	...
RR Tau	A2e	4.23	Y	8,15	+200	Na I	15	III	e	...	6.12	60	24
VV Ser	A2e	1.52	Y	7,8	+150:	Na I	11	III	...	...	7.38	85	24
HK Ori	A3-4e	2.2	Y	8	+150:	Na I	11	III	e	...	7.4	175	24
BF Ori	A5e	2.5	Y	4,8,29	+150:	Na I	16	III	e	e:	6.58	80	24
KK Oph	A5e	2.2	...	8	+150:	Na I	17	III	e	...	6.9	85	24
T Ori	A5e	2		8,29	+150:	Hβ	18	III	...	...	C	130	23
V351 Ori	A7III	2.9	...	30	+150	Hα	30	IP/III	...	...		...	...
CQ Tau	F2e	2.2	Y	4,8,29	+90	Hα	15	IP	e/III	...		...	...
HAeBe Stars with Outflow and Accretion:													
HD 50138	B8e	0.3	Y	6	+400	C IV	10	III	III/I	IP	7.17	150	10
HD 100546	B9e	$\geq$0.08	...	11	+400	C IV	11	III	IP	IP/I	8.63	250:	11
NX Pup	A1IIIe	1.7	...	29	+150	Mg II	11	III	III	...	7.03:	120	24
Main Sequence Stars with Accreting Gas													
HD 176386	B9	0.1	...	26	+300	C IV	19	abs	abs	abs	0.5	220:	19
HD 37062	B1.5e:	1.7	...	26	+400	C IV	11	abs	abs	IP	C:	250:	11
V372 Ori	A0	Y	...	26,29	+350:	C IV	11	abs	abs	abs	5.33:	...	...

3.2. *Stars with veiled spectra, stars lacking circumstellar dust, and stars with low S/N data*

Four of our program stars (HD 53367, HD 52721, HD 76534, and ω Ori), with IR excesses consistent with free-free emission rather than circumstellar dust (Hillenbrand et al. 1992), show wind activity typical of normal or classical Be stars of the same spectral type. These stars will not be discussed further. HD 97048, a star with a prominent IR excess due to circumstellar dust, has heavily veiled UV spectra, precluding line analysis. Z CMa and BF Ori are represented in the IUE archives by extremely low S/N mid-UV high dispersion spectra, which are of too poor quality for further analysis. Spectra of a number of these stars are shown in Imhoff (1994).

3.3. *Stars with spectral signatures of accreting gas*

While the early UV studies of HAeBe stars preferentially selected stars with optical signatures of outflowing material, largely to avoid confusion with classical Be stars, such a strategy excludes the majority of HAeBe stars which exhibit double-peaked (type III) P Cygni emission in Hα (Finkenzeller & Mundt 1984). Several recent studies of selected HAeBe stars with double-peaked Hα emission (Grady et al. 1993a; HR 5999 Pérez et al. 1993a; Graham 1992; Welty et al. 1992; Grinin et al. 1994; Grady et al. 1995) have demonstrated that at least some of these stars exhibit optical or UV signatures of accreting gas in transitions of one or more elements and ionization stages. In contrast to outflowing material, accreting gas in the UV manifests, either as inverse P Cygni profiles characterized by emission shortward of line center with absorption longward of line center, or absorption which is systematically enhanced longward of line center (Fig. 1). As in the case

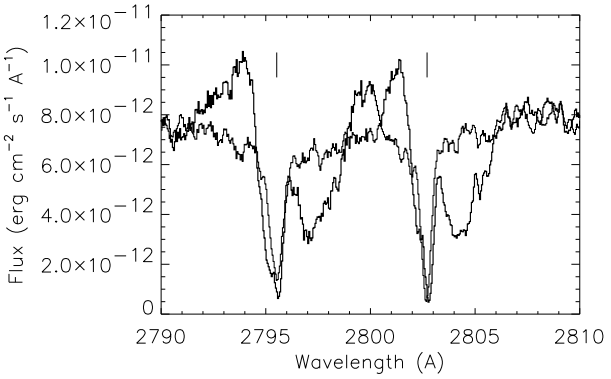

Fig. 1. An example of accreting, circumstellar gas in a Herbig Be star: HD 100546. The Mg II resonance transition for HD 100546 (bold) and the main sequence B-shell star 51 Oph, with both spectra from 1995 March. The HD 100546 line profile is characterized by emission shortward of the transition rest wavelength, a strong, and resolved, absorption feature near the estimated stellar radial velocity, and a prominent absorption component at longer wavelengths. Despite a 2:1 ratio in the oscillator strengths of the two transitions in the Mg II resonance doublet, the high velocity features have comparable absorption depth, suggesting that the absorption is optically thick. In contrast, 51 Oph, a Main Sequence Be-shell star with circumstellar dust, which has previously been reported to show low velocity accreting gas, primarily in species such as C IV, lacks the conspicuous emission and the high velocity absorption component

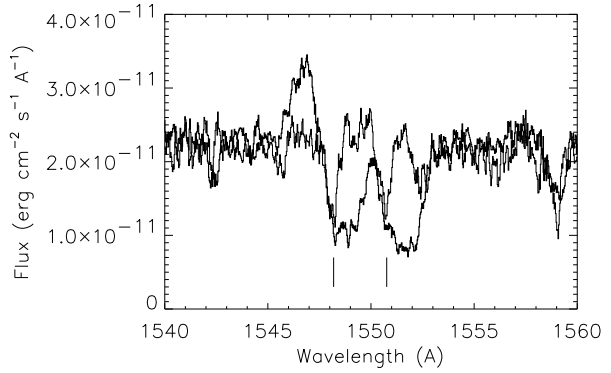

Fig. 2. Accreting gas in C IV for HD 100546 and 51 Oph

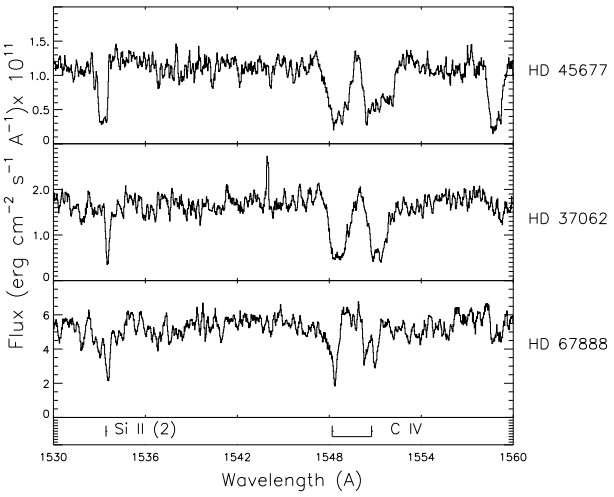

Fig. 3. Far UV high dispersion spectra covering C IV (1) at 1548 and 1552 Å and Si II (2) at 1533.432 Å for HD 45677 (B2[e]) from 1994 December 12, HD 37062 (B1.5e) from April 26, 1981, and HD 67888 (B4e) from 1987 June 22

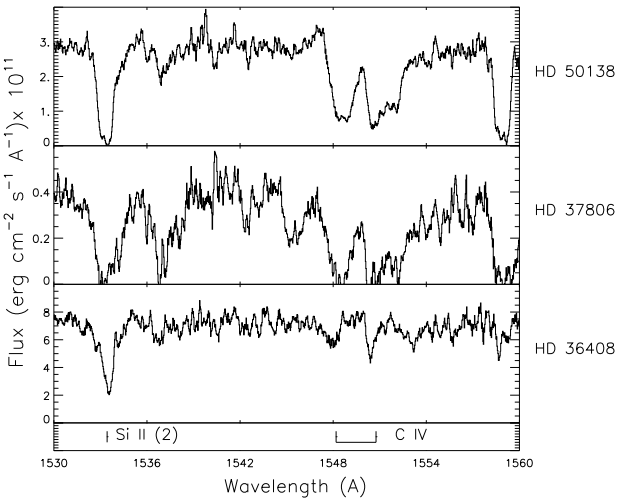

Fig. 4. C IV and Si II for the B8-B9e stars: HD 50138 (B8[e]) from 1994 December 12, HD 37806 (B8e),and HD 36408 from 1986 October 6

of the stellar winds, the HAeBe stars with accreting gas signatures have absorption in transitions and species not commonly observed in the spectra of main sequence stars of comparable type (e.g. C IV, Fe III (34)), or which is much stronger than is typical for the spectral type (Figs. 1, 2).

As is commonly done in estimates of stellar wind properties, maximum accretion velocities can be estimated either from the long wavelength edge of the absorption feature, for transitions with a comparatively rapid return-to-continuum, or from the return to continuum level for the features with softer profile edges.

When all of the archival and recent IUE observations are examined, we find 12 HAeBe stars with UV spectral signatures of accreting gas in at least some of their spectral lines (Figs. 3-13). For the earliest spectral types in our survey, accretion signatures are concentrated in species such as C IV, Si IV, Al III, and Fe III. Species which would not be expected to be present in the photospheric spectrum of a main sequence star of comparable spectral type tend either to not have absorption features, or to have absorption in only transitions to the O eV level of the ground

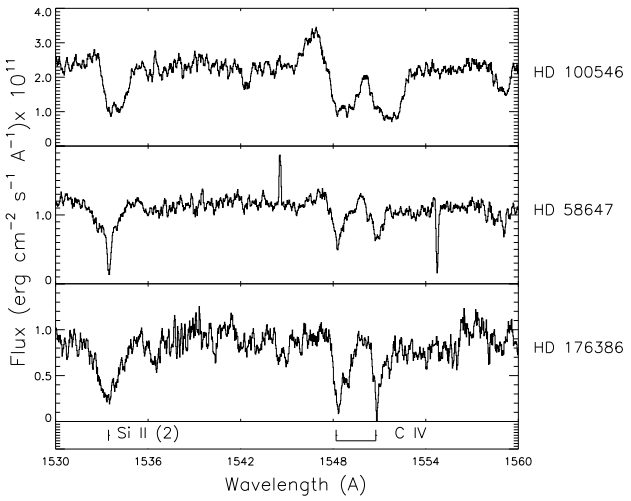

Fig. 5. C IV and Si II for B9e stars HD 100546 from 1995 March 7, HD 58647 from 1994 December 12, and HD 176386 from 1992 September 24

configuration (e.g. Fe II(1)) suggesting an origin in the foreground interstellar medium, rather than in circumstellar gas. For the later-type stars in our sample, accreting gas signatures are present in lower ionization species, and may dominate the mid-UV spectrum (e.g. HR 5999, Pérez et al. 1993a). Detection of accreting material in 36% of the HAeBe stars with high dispersion data demonstrates that accretion signatures are not rare in the spectra of intermediate-mass PMS stars. Furthermore, accretion signatures are not restricted to the HAeBe stars with IUE high dispersion spectra. Accretion in optical line profiles has been reported in spectra of an additional 8 HAeBe stars and can be inferred by intercomparison of our data with previously published line profiles for VV Ser and HK Ori (see Table 3).

However, our detection rate falls well below the 85% noted in optical studies of classical T Tauri stars (Edwards et al. 1994) raising the possibility of significant differences in the near-stellar envelopes of these stars. We note, however, several selection effects in the UV high dispersion data. First, the IUE data are strongly biased toward the optically brightest HAeBe stars, and thus toward those with minimal foreground extinction. Any archival dataset is also subject to the research interests of the original investigators. Thus, the IUE observations, particularly the earlier spectra, are skewed toward the HAeBe stars with P Cygni profiles at Hα, despite the fact that such objects do not form a majority of the stars cataloged either by Finkenzeller & Mundt (1984) or more recently by Thé et al. (1994). This bias in the available UV data has not been compensated for by HST observations; to date only one HAe star, HD 104237, has been observed by the HST GHRS (Brown 1996, private communication). Optical surveys of both HAeBe and classical T Tauri stars go significantly fainter than can be achieved with the IUE, and thus include objects which are more heavily embedded, or even viewed only as reflection nebulosity (e.g. HL Tau, Stapelfeldt et al. 1995).

3.4. *Accretion in non-emission line A and B stars*

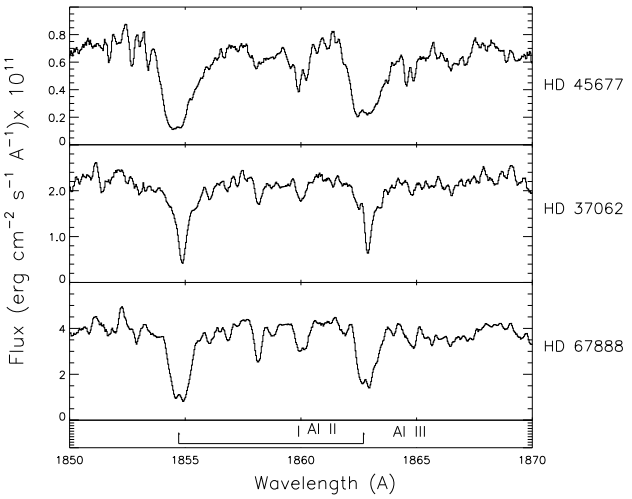

Fig. 6. Al III profiles for the Herbig Be stars shown in Fig. 3

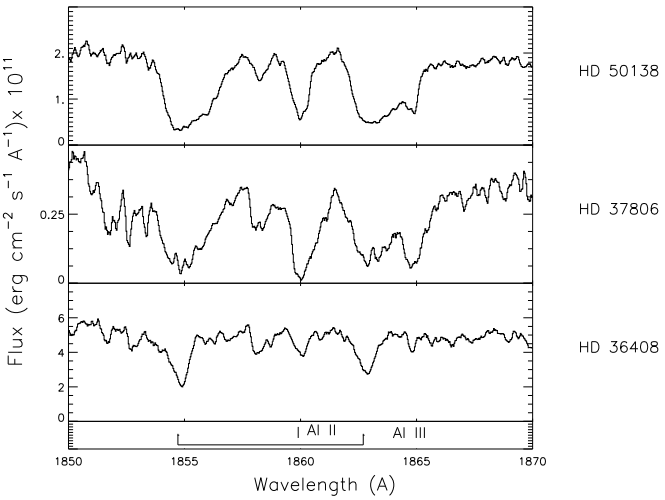

Fig. 7. Al III profiles at B8-9e for the stars shown in Fig. 4

In addition to the emission line objects, the IUE archives contain spectra of a number of the non-emission line objects considered in the catalog of Thé et al. (1994). As a group, these stars have less dramatic UV spectra than the HAeBe stars, and tend to have predominantly absorption line spectra. As is the case for the main sequence A-shell stars (Grady et al. 1996), the mid-UV spectra of these stars, at the 6−9 Å resolution of the IUE low dispersion spectra, correspond to objects 2-3 subtypes later than

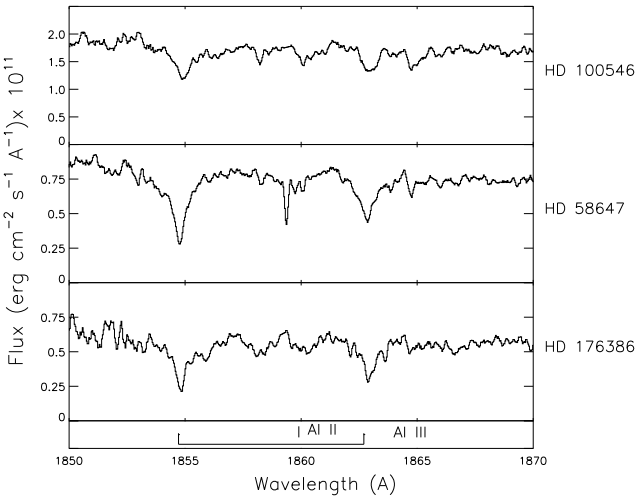

Fig. 8. Al III profiles at B9e for the stars shown in Fig. 5

those inferred from their optical data, or from the FUV spectral energy distributions. When viewed at the 25 km s^{-1} resolution of the IUE high dispersion data, these stars show strong, frequently saturated absorption concentrated at low velocity. In some cases (e.g. HD 176386) asymmetric higher velocity absorption is detectable in Mg II, but is more prominent in the FUV Fe III (34), C IV, and Si IV transitions. For the stars with strong, but resolved, absorption features at comparatively low velocities, the presence of accreting gas can be inferred, by the systematic trend of Fe II absorption centroids to higher, positive velocities with increasing excitation. This technique is also applicable to main sequence stars, such as β Pic and other A-shell stars (Grady et al. 1996), at the resolution of the IUE. Apart from β Pic, the first non-emission line, but plausibly young, A/B star with accreting gas detected in IUE data was HD 176386 (Grady et al. 1993b). Inspection of the IUE data for stars from the list of non-emission line "shell" stars in Thé et al. (1994) reveals the presence of accreting gas in 2 additional objects. The locations of HD 176386 (near TY CrA in the CrA star formation region), HD 37062 (also known as V361 Ori), and V372 Ori in Orion, suggest that these stars are young. The strength of the accreting gas profiles seen in the IUE data suggests that the gaseous accretion rates are similar to that seen toward β Pic.

Accretion signatures are also found in UV spectra of a few stars, such as 51 Oph (Grady & Silvis 1993), historically identified as classical Be stars, and in a number of A shell stars (Grady et al. 1996). In these stars, the accreting gas can only be followed, at the resolution and S/N of the IUE, to $+100 - +130$ km s^{-1}. With the exception of 51 Oph, these stars typically have smaller IR excesses at 12 μm than β Pic and in some cases Vega-like excesses. The star, β Pic thus appears intermediate in accretion characteristics and in IR excess between the PMS HAeBe stars and the field A shell stars. The similarity to the young main sequence stars identified in our survey lends support for interpreting β Pic as either a zero-age or young main sequence object (Lanz et al. 1995) rather than a system with an age of a few 100 Myr (Paresce 1991).

4. The accreting circumstellar gas in HAeBe and young intermediate-mass stars

In this section we discuss the accreting gas detections beginning with the accretion velocities seen, the presence of accreting, neutral gas at unexpectedly high velocities, variability of the accreting material and the presence of multiple absorption components which are similar to features seen in the spectra of β Pic, and the presence of ionic species which can be produced only by collisional ionization of the accreting gas.

4.1. *Velocity fields in HBe stars*

Accreting gas is detectable at the S/N of our IUE spectra to $+300-400$ km s^{-1} in 5 Herbig Be stars in our sample with data coverage over the entire IUE wavelength range. Accreting material with velocities as large as $+500$ km s^{-1} has previously been reported for R CrA (Graham 1992), and is seen in 3 of the program stars from the Thé et al. (1994) catalog listed as shell stars with no net Hα emission (HD 176386, Grady et al. 1993b; HD 37062; V372 Ori). Lower velocity (to $+200-250$ km s^{-1}) accretion is detectable in one star, HD 58647, which Thé et al. (1994) reported as having no emission. Our ESO data, however, clearly shows type III emission in Hα. All of these stars have higher column densities of accreting gas, which can be followed to higher velocities that are seen in Be stars with IR excesses consistent with dust, such as 51 Oph. The available IUE data for this group of stars are sufficiently sparse that we cannot determine whether the difference in accretion signatures reflects episodic enhancement in the mass accretion rate in objects like HD 176386 or real, systematic differences between these stars. Figures 3-8 show the regions near C IV and Al III for the program HBe stars. Figures 9-13 show the Mg II region for those program HBe stars with high dispersion mid-UV spectra.

4.2. *Velocity fields in HAe stars*

For the HAe stars our UV high dispersion coverage is largely restricted to the mid-UV, limiting our coverage in terms of both ions and ionization stages. We find accreting gas in Fe II and Mg II to more than $+150$ km s^{-1} in 6 cases (Figs. 9-13). Accreting gas is visible in Hα for some of the program stars (Figs. 14-16), and is particularly prominent in Na I where it is detectable to between $+150$ and 300 km s^{-1} in Na I or He I (Figs. 17-19). Similar accreting material has been reported in WW Vul, RR Tau, and CQ Tau (Grinin et al. 1995), BF Ori (Welty et al. 1992), KK

Oph (Hamann & Persson 1992), T Ori (Ghandour 1994), and in VV Ser (Chavarría-K et al. 1988; Finkenzeller & Mundt 1984). Intercomparison of our observations with line profiles in the literature suggests that variability in the accreting gas, especially at high velocity, is ubiquitous. Lower velocity accreting material is detected in HD 35929 out to +100 km s^{-1}. In short, the available optical and UV data are consistent with detection of accreting, circumstellar gas over essentially the same velocity range as is observed in the β Pic system (Vidal-Madjar et al. 1994 and references therein).

Velocity fields of several hundred km s^{-1} are routinely detected in optical spectra of classical T Tauri stars (Edwards et al. 1994), and have historically been interpreted as detection of material in free-fall toward the star (Walker 1972). Overall, we find no trend of increasing accretion velocity with earlier spectral type (increasing stellar mass); instead we find that the highest velocity accretion signatures are seen in the spectra of stars with especially prominent IR excesses, as measured by the IRAS excess at 12 μm.

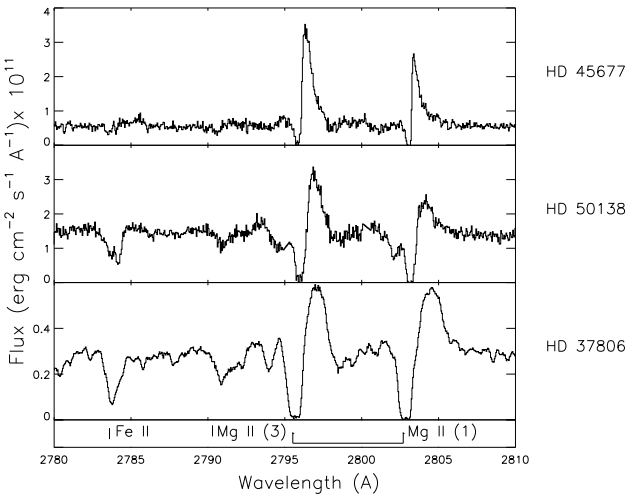

Fig. 9. Mg II profiles for Herbig Be Stars. HD 45677, HD 50138, HD 37806

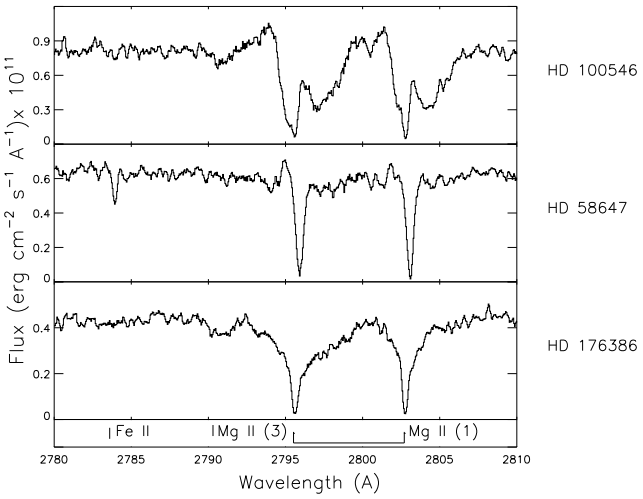

Fig. 10. Mg II profiles at B8-9e: HD 100546, HD 58647, and HD 176386

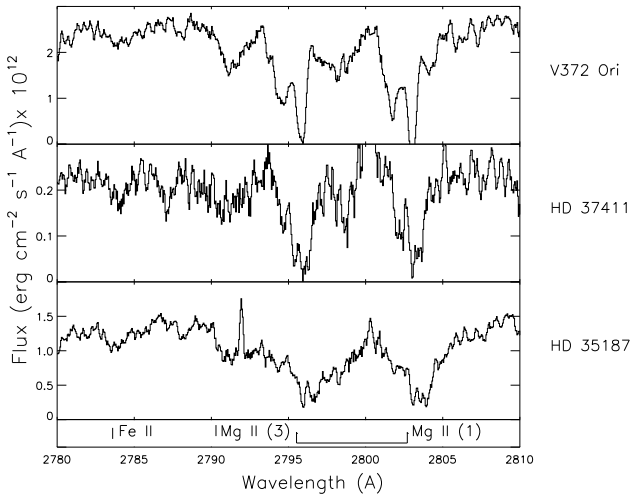

Fig. 11. Mg II at B9-A2e: V372 Ori (B9e+A0e), HD 37411, and HD 35197

4.3. *Presence of accreting neutral gas*

Grinin et al. (1994a,b, 1995) have noted the presence of neutral, atomic gas, visible in Na I out to +150-250 km s^{-1} in the line of sight toward 2 Herbig Ae stars, UX Ori and RR Tau. They note that the photoionization lifetime for neutral species deep in the gravitational well of an early A star is at most a few seconds, and thus that the atomic gas must be produced in situ at high velocity from either the dissociation of molecules, or, for more refractory elements, sublimation of grains. The wavelength coverage of our IUE data permits us to extend the atomic gas surveys to Mg I and for the Herbig Be stars to C I (2) and O I (2). Our detections of accreting, neutral, atomic gas are indicated in Table 4. We find that earlier than B8 in spectral type, the atomic gas features are typically weak, exhibiting absorption consistent with the velocity resolution of the IUE and without excess absorption on the red wing of the line profile. We tentatively identify these features as absorption from foreground interstellar gas and will not discuss them further.

Beginning at B8, and continuing to later spectral types, the combined IUE and optical high dispersion data indicate that neutral, atomic gas is seen, not only at the system velocity, but also, in the majority of our program stars in the accreting material as either an enhanced red wing (Mg I and Na I) on the profile, or in some cases with enhanced absorption features similar to the Ca II and Fe

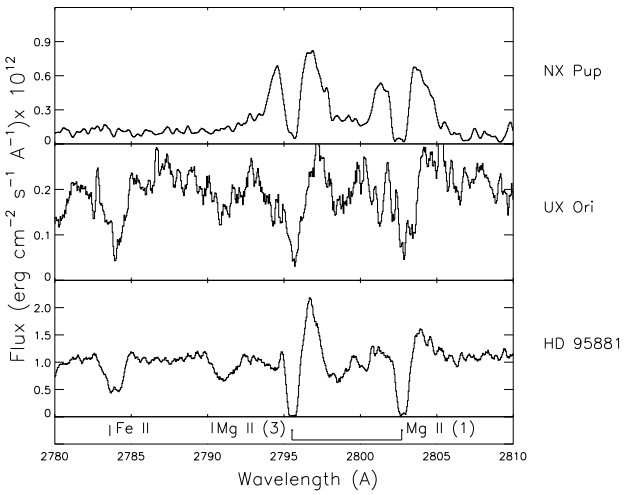

Fig. 12. Mg II profiles for Herbig Ae Stars. **a)** NX Pup (A1-3 IIIe), UX Ori (A1-3IIIe), and HD 95881 (A2e)

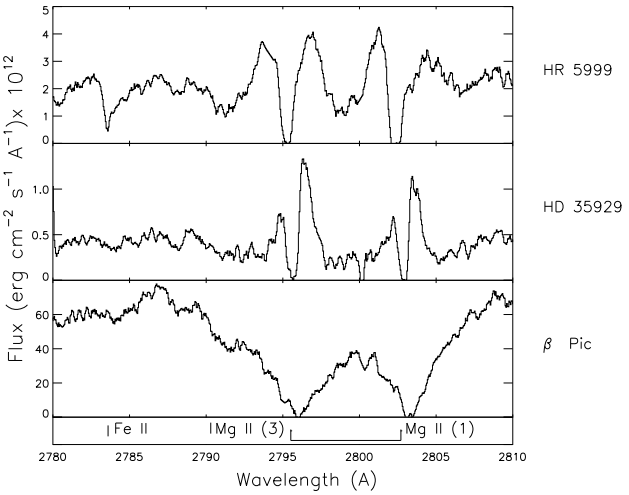

Fig. 13. Mg II profiles for HR 5999 from the optical maximum observation of 1990 September 7, HD 35929 from 1994 Jan. 12, and a representative IUE spectrum of β Pic for comparison

II profiles in β Pic. The low velocity absorption in the spectra of these stars is likely to contain both foreground interstellar and circumstellar components which cannot be separated in the IUE data. He I 5876 which was observed in the same spectra as the optical Na I data, lacks the prominent absorption feature at the system velocity, and shows red-asymmetric absorption. In some cases (NX Pup), prominent inverse P Cygni profiles are present. Accreting, neutral gas is visible in our program stars from +70 to +300 km s^{-1}. The available optical data, together with our observations and the UV spectra demonstrate that the neutral gas column densities are strikingly variable on timescales as short as night to night.

The majority of the program stars with accreting gas have type III P Cygni profiles in Hα characterized by double-peaked emission with a central absorption reversal (Figs. 14-16). At the resolution of the ESO data the depth of the absorption reversal usually does not go below the local continuum level. However, the absorption reversal, rather than being the approximately Gaussian feature seen in classical Be star spectra, consistent with formation of the entire line profile in gas which is rotating in Keplerian orbit about the star, is frequently asymmetric or shows secondary emission peaks. Prominent enhancements of the absorption on the red side of the emission profile are seen in our spectra of T Ori and UX Ori. Similar features have been reported in differenced spectra at Hβ by Ghandour et al. (1994).

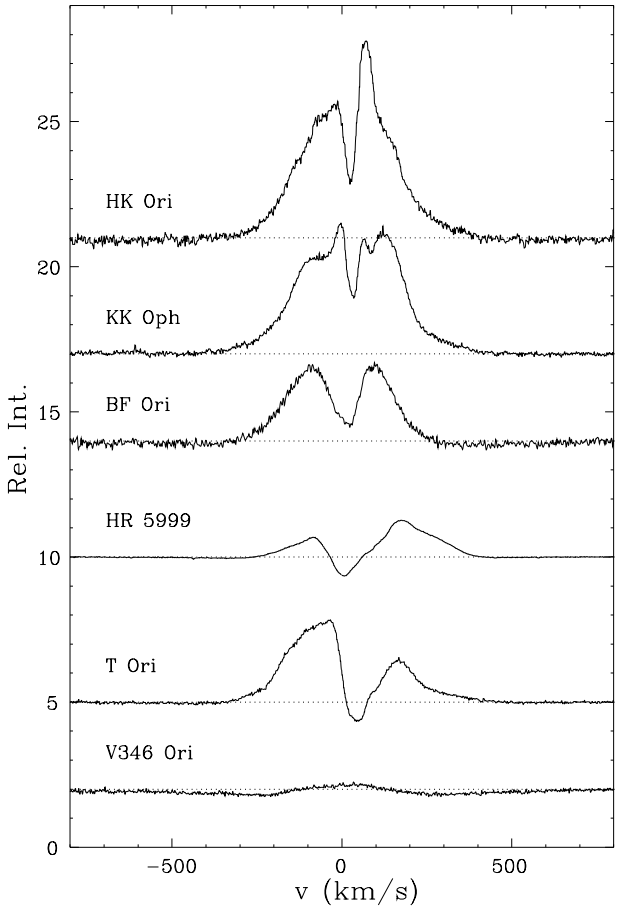

Fig. 14. Selected Hα profiles for our ESO program stars

The IUE data suggest that high velocity, accreting atomic gas is routinely observed in the more cosmically abundant elements in the circumstellar gas of HAeBe stars, with accretion signatures in more highly ionized material. Detection of such accretion in Na I prompted Grinin et al. (1994) to suggest a link with grain sublimation in UX Ori which is supported by the detection of an increase in the 2−13 μm IR excess at optical minimum

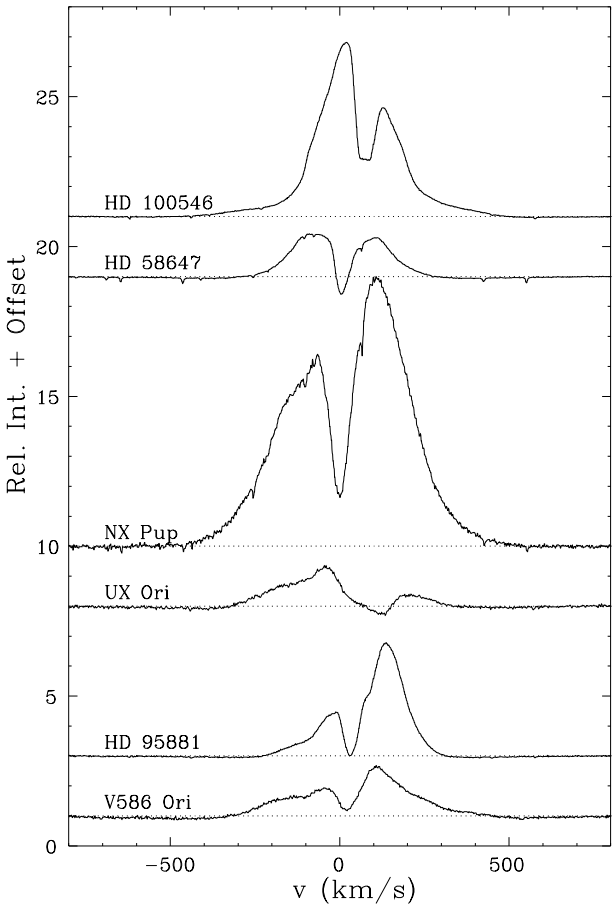

Fig. 15. Selected Hα profiles for our ESO program stars, continued

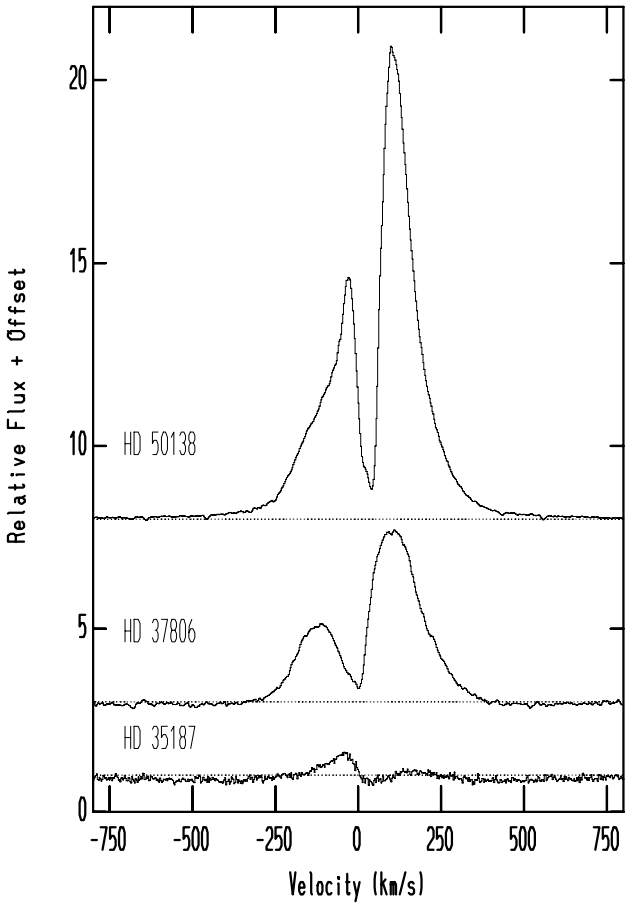

Fig. 16. Selected Hα profiles for our Ritter Observatory program stars. Offsets added to the 3 spectra were 7, 2, and 0, respectively. The dotted line indicates the estimated local continuum level

(Hutchinson et al. 1994). Detection of increases in the IR excess at optical light minima have now been reported in one HBe star, HD 45677 (Sitko et al. 1994), and are potentially present in one other object, AK Sco (Hutchinson et al. 1994). Given the limited IR photometry for these stars at different epochs, detection of such variation in three systems suggests that the near-IR excesses of these objects are highly variable.

4.4. *Structure in the line profiles and variability*

In addition to the well-monitored HAe stars with strong stellar winds, HD 163296 and AB Aur, 7 of the program stars with accretion detections have UV high dispersion spectra from multiple epochs. With the exception of HD 37806 and HD 35929, all of the program stars with multiple observations exhibit striking changes in the high velocity accreting gas from observation to observation. In the case of HD 100546 (Fig. 20) and HD 95881, singly ionized species such as Mg II, Cr II, Mn II, Fe II, Si II, Al II, C II, and Zn II show prominent absorption components with typical FWHM of $\sim$50 km s^{-1} centered near 100 km s^{-1}, in the highest accretion state spectra in addition to the saturated absorption features centered on the stellar radial velocity which is present in all spectra. In the case of the Fe II transitions, the prominence of this velocity component increases with excitation. The overall appearance of these velocity components is similar to the features routinely observed in Na I. The sparse nature of the IUE observations does not permit us to address the time scale of variation of the UV features. However, night-to-night optical observations at Na I and Hα (de Winter 1996) demonstrate that the time scale for variability at high velocity is clearly shorter than 24 hours. Similar profiles with night-to-night changes in R CrA prompted Graham (1992) to suggest that accretion toward HAeBe stars is clumpy rather than continuous. The overall appearance of these profiles, except for the greater strength of the absorption, the trend of increasing excitation and/or ionization in the higher velocity gas, and the timescale for variation is similar to the high velocity components seen in optical and UV spectra of β Pic where such spectral features have been modelled as the gaseous comae and bowshocks of infalling,

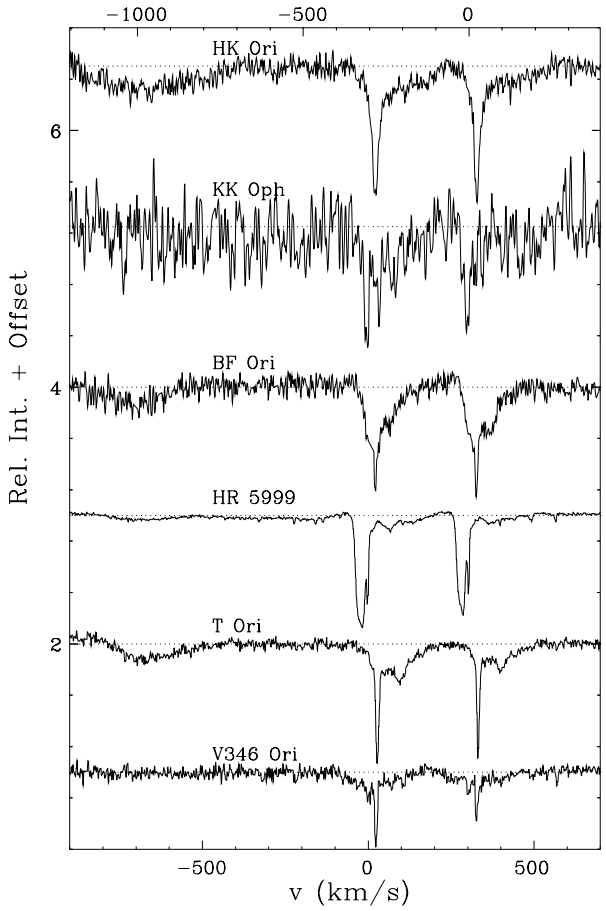

Fig. 17. Selected NaI and He I 5876 Å profiles for the stars from Fig. 12. The rest wavelength for the He I feature corresponds to -725 km s^{-1} on the velocity scale of the Na I feature

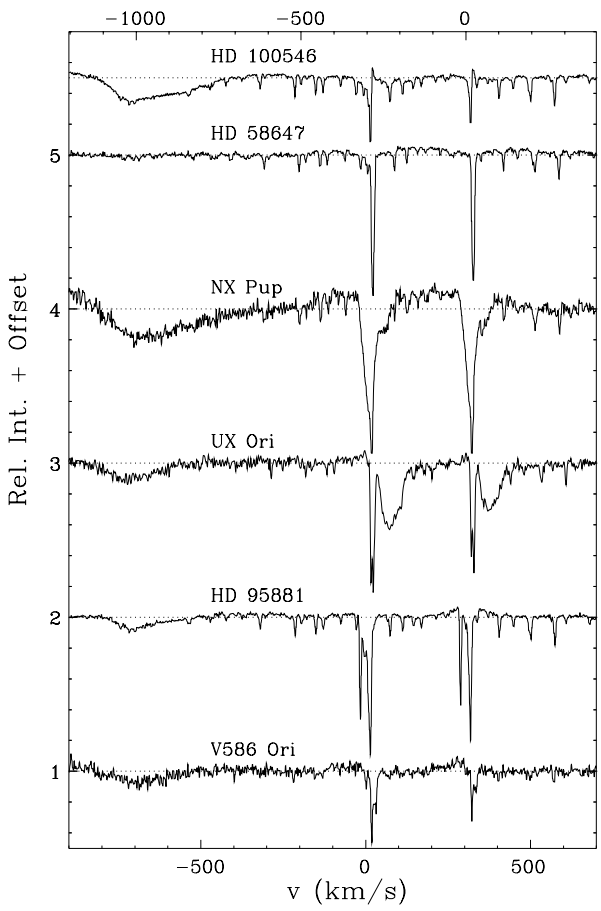

Fig. 18. Selected NaI and He I 5876 Å profiles for the stars from Fig. 13

evaporating bodies (Beust & Lissauer 1995 and references therein).

The comparatively low resolution of the IUE data together with S/N limitations and the heavy line blanketing, particularly in Fe II, makes detection of similar absorption components within 40 km s^{-1} of the system velocity challenging in individual line profiles. However, by intercomparing transitions covering either a range of excitation (Fe II) or ionization, we can infer the presence of low velocity absorption components in objects like β Pic and our HAeBe program stars. We infer the presence of low velocity absorption components in UX Ori, HD 95881, HR 5999, and HD 37411. For the Herbig Be stars in our sample transitions of Al III and Fe III (34) can be used to hunt for absorption components. The available data suggest that such features are routinely detected at low and intermediate velocities in the accreting gas of the majority of our program stars.

4.5. *Collisionally ionized gas - C IV*

Where we have FUV spectra, C IV absorption defining the highest velocity accretion detected to date is seen in all of the program HBe stars. Similar absorption is seen in HD 176386, HD 37062, V372 Ori, and the "classical" Be stars with accretion signatures. The strength of the C IV absorption is larger than that seen in the majority of classical Be stars of comparable spectral type, and is present in stars with lower v sin i than would be expected to show the transition (Grady et al. 1987; Grady et al. 1989). With a few exceptions, classical Be stars do not routinely exhibit UV spectral signatures of high velocity accretion (Grady et al. 1989), suggesting that the features seen in our program stars are not related to the Be-phenomenon. As noted by Marlborough & Peters (1986), the presence of C IV absorption in the spectrum of a B star is unexpected later than B2 and is consistent with collisional ionization of the circumstellar gas. C IV emission is typically not seen in any "classical" Be star. Usually the C IV and Si IV absorption in our program stars peaks at higher positive velocities than the lower ionization material, frequently in the vicinity of the locally enhanced absorption

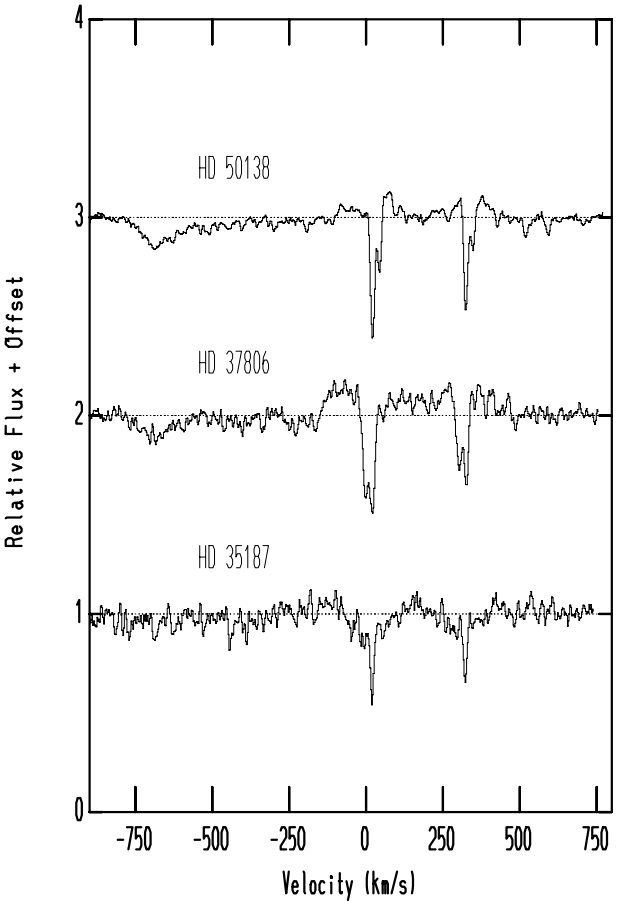

Fig. 19. Selected NaI and He I 5876 Å profiles for the stars from Fig. 14

features seen in species such as Fe II or Fe III. The velocity range and appearance of the C IV profiles is similar to the C IV absorption noted in β Pic (Vidal-Madjar et al. 1994).

In contrast to "classical" Be stars, several of the program HAeBe stars, including HD 104237, exhibit emission in C IV. Of the stars with accreting gas, HD 100546 shows variable C IV emission and absorption profiles. The bulk of the spectra show inverse P Cygni profiles in C IV, with, however a range of emission strength; the 1995 March spectrum (Figs. 2, 5) is the maximum emission spectrum observed to date. The 1993 April observation, in contrast to the other spectra shows weak type I P Cygni emission not only in C IV but also Si II and Al II. HD 50138 (Fig. 4) intermittently shows a similar, but weaker feature, which is particularly prominent in early data. HD 37062 shows a trace of emission in one of three IUE observations. For these stars the weakness of the emission, relative to the equivalent width of the absorption, precludes formation of the accreting gas in a spherical envelope, but instead implies that the bulk of the C IV absorption is in our line of sight. Several other HAe stars have C IV emission detectable in low dispersion spectra (HR 5999, HD 35929, and HD 144432). HST observations will be needed to determine whether the emission in these stars resembles transition region features expected for cooler objects, or is unambiguously associated with the accreting gas.

Table 3. Detection of Accreting, Neutral Gas in HAeBe Stars. The lines surveyed include O I (2)λ1302, C I(2)λ1657, Mg Iλ2852, and He Iλ5876. Lines showing redshifted absorption are indicated by X; IP indicates the presence of inverse P Cygni profiles with emission on the blue wing of the line and absorption redward of line center. Notes: 1) our data show high accretion state, 2) our data show variable accretion states, 3) our data show low accretion state, high accretion state is in literature, 4) data from literature, 5) variability noted in literature, 6) Graham (1992, private communication), 7) Graham (1992), 8) Morrison & Beaver (1995), 9) Grinin et al. 1994, 10) Grinin et al. 1995, 11) Finkenzeller & Mundt (1984), 12) Hamann & Persson (1992)

Star	O I (2)	C I(2)	Mg I	Na I	HeI	Notes
HD 45677	em	IS	abs	e	IP	2,6
HD 37062	IS	IS	IS	...	...	1
R CrA	...	...	...	IP	IP	4,5,7
HD 50138	abs	abs	X	e	X	2,5,8
HD 37806	abs	abs	abs.	...	...	1
HD 100546	X	X	X:	IS	X	2
HD 58647	IS	IS	IS	...	...	
HD 176386	IS	IS	IS	...	...	1
UX Ori	...	...	X	X	X	2,9
NX Pup	...	...	X	X	I/IP	2
WW Vul	...	...	...	X	?	4,10
RR Tau	...	...	...	X	X	4,5,10
VV Ser	...	...	...	X	X	3,11
HD 95881	...	abs	X	e	...	2
V586 Ori	...	...	...	IP:	IP	2
HK Ori	...	...	...	X	X	2
KK Oph	...	...	...	X	...	2,12
BF Ori	...	...	...	X	X	4,5,10
V346 Ori	...	...	...	IS	...	
T Ori	...	...	...	X	IP	1
HR 5999	e	...	X	X	X	4,5

4.6. *Collisionally ionized gas - lower ionization species*

For the HAe stars in our sample, lower ionization species such as Al III (Bruhweiler et al. 1989) provide tracers of collisionally ionized gas similar to C IV for the HBe stars. For the late HBe stars with both FUV and mid-UV high dispersion spectra, we find absorption in Al III and Fe III (34) over much the same velocity range as for C IV. Beginning at B8-9 and continuing to A3-4, Mg II (3) absorption is detectable at 2790.3 Å in HD 50138 and HD 95881. Typically this absorption exhibits a sharp onset and gradually weakens with increasing wavelength, with the absorption redward of the system velocity. The absorption in Mg II (3) can be followed out to +300 km s^{-1} in HD 50138, sampling essentially the same velocity range as the Al III and Fe III (34) absorption. Thus, the line

provides a suitable mid-UV probe of the higher velocity collisionally ionized/excited gas in these stars. Similar absorption features are seen in HD 37806 (Fig. 9), HD 176386 (Fig. 10), V372 Ori, HD 37411 (at low S/N), and in HD 35187 (Fig. 11), HD 95881, and UX Ori (Fig. 12). By A5 the increasing strength of the photospheric Mg II absorption causes the Mg II (3) features to blend with Mg II (1), although the feature may be present in the spectrum of HR 5999 (Fig. 13). However, the available data suggest that plasma which has been collisionally ionized is routinely present in the accreting circumstellar gas of HAeBe stars and is preferentially concentrated toward the higher velocities. Similar behavior has been reported for β Pic (Vidal-Madjar et al. 1995 and references therein).

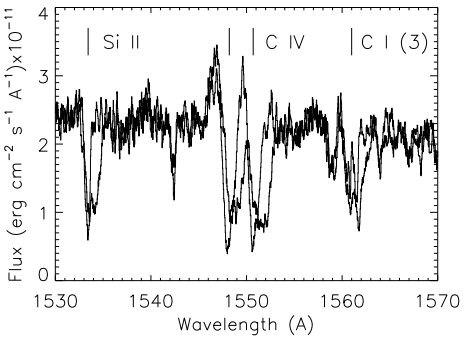

Fig. 20. Variation of the high velocity, accreting gas in HD 100546 between 1995 March 7 (bold) and 1995 May 25. Leader lines indicate the location of lines of Si II (2), C IV (1), and C I (3) which are particularly variable

5. Covering factor of the gas

Intercomparison of the numerous Fe II transitions in the mid-UV, the Na I D doublet, C I multiplets 2-5 in the FUV (where available), together with C IV and Mg II, and the Si II transitions suggests that the high velocity, accreting gas is typically optically thick, with all members of a doublet or multiplet having comparable equivalent width in absorption. A number of these profiles have absorption which has constant depth over 50 km s^{-1} or more in 2 or more transitions which differ by a factor of 2 or more in f-value. We interpret these flat absorption troughs as detection of optically thick, saturated absorption which does not fully cover the star. The covering factor can be estimated, then from the absorption depth relative to the continuum. Grinin et al. (1995b) have used a similar technique in analyzing circumstellar Na I profiles toward 2 Herbig Ae/Be stars, UX Ori and RR Tau, and find covering factors for the high velocity Na I of order 30%. Our detections of high velocity Na I absorption suggests that covering factors in the range 15−30% are common among the Herbig Ae stars. We find comparable covering factors for C I in the B8-A2 stars with FUV high dispersion data. The filling factor of the singly ionized, accreting gas is typically somewhat higher, usually between 30 and 50% for Si II and Fe II. The C IV absorption is especially prominent with covering factors between 30−60%. For a typical PMS intermediate mass star with R =3 $R_\odot$, this corresponds to cloud sizes of order $10^6 - 10^7$ km, comparable to the size of Lyα comae in Solar system comets at 1 AU. The bulk of the accreting gas, however, if we assume that the velocities originate in material in free-fall, comes from within 0.25 AU of the star ($v \geq 100$ km s^{-1}) for the lower ionization species and within 0.15 AU for the higher velocity material, implying that the gas clouds are appreciably larger than Sun-grazing comets at comparable distances from the Sun.

6. Correlation with v sin i

Thirty of the program stars, including 25 HAeBe stars, have measured projected stellar rotational velocities, v sin i. These measurements are available typically for HAeBe stars with modest Hα emission, and minimal optical veiling. v sin i data are taken from the compilation of Hillenbrand et al. (1995) except for HD 37062, HD 58647, and HD 100546. Estimated uncertainties in the v sin i data are of order 20−30 km s^{-1}. For the most part, the measurements of Hillenbrand et al. are in agreement with the measurements of Böhm & Catala (1994), except for UX Ori and RR Tau. The photospheric absorption wings of Mg II in the mid-UV high dispersion spectrum of UX Ori suggest a v sin i near 150±10 km s^{-1}, in agreement with optical estimates by Grinin (1995, private communication). We therefore adopt the value of 175 km s^{-1} from Hillenbrand et al. (1995) in favor of the lower v sin i measurement from Böhm & Catala (1994). Similarly, optical data for RR Tau near optical maximum light suggest a higher v sin i than the value of 60 km s^{-1} measured by Hillenbrand et al. (1995). For this star, therefore, we adopt the value of 170 km s^{-1} from Davis et al. (1983).

6.1. *New v sin i estimates*

Three of our program stars have mid and far UV spectra which are sufficiently minimally line blanketed by circumstellar gas features (primarily Fe II), and which have spectral S/N sufficiently high to enable us to compare their spectra with rapidly rotating B and Be stars with v sin i measured by Slettebak (1982). In the case of HD 58647 we find good agreement with a spectral type of B8-9 and a v sin i comparable to HD 93563. For HD 37062, comparison of Si III (4) absorption and phospheric features in the vicinity of Si II (2) suggests a significantly earlier spectral type than the optical type of B5 from SIMBAD. We find reasonable agreement with the photospheric absorption for a UV spectral type of B1.5 and v sin $i \approx 250$ km s^{-1}. For HD 100546, our data suggest a reasonable

agreement with a spectral type of B9 and v sin i=250–280 km s^{-1}.

6.2. *Trends with v sin i*

Previous studies of spectral characteristics and photometric variability in HAeBe stars have not shown any trends with v sin i, largely due to omission of any dependence on spectral type (Finkenzeller 1985; Herbst et al. 1994). When accretion and outflow signatures are displayed as a function of both spectral type and v sin i, we find that the stars with accretion signatures, at any given spectral type, tend to cluster toward higher v sin i than do the objects with outflow signatures (Fig. 19). Stars which have shown both outflow and accretions signatures (HD 50138) and prominent changes in the appearance of Mg II (type I to type III, e.g. HD 163296) are located at intermediate v sin i. Similarly, AB Aur, for which Marsh et al. (1995) have detected spatially extended IR emission suggestive of a disk viewed close to edge-on, but which shows outflow signatures in all optical and UV spectra (Praderie et al. 1986), also has an intermediate v sin i. At the earliest spectral types, v sin i $\geq$200 km s^{-1} appears to be necessary for detection of accretion, whereas by mid-A, v sin i in excess of 85 km s^{-1} suffices. However, the v sin i range for which accreting material is seen corresponds to stars which would be considered comparatively rapid rotators *if they were on the Main Sequence at that spectral type.* The range in v sin i where accreting gas is detected in the HAeBe stars is similar to the range occupied by the Main Sequence A stars with "shell" spectra, that is the presence of narrow absorption features due to low ionization circumstellar gas. Our data suggest, therefore, that by the time the line of sight to the star is sufficiently unobscured to permit measurement of v sin i, the HAeBe stars closely resemble Main Sequence stars in their rotation rates. The v sin i data and the accretion detections by themselves do not permit us to distinguish between a trend of preferential detection of accreting gas toward more rapidly rotating stars and a correlation with stellar inclination, in which accreting gas is preferentially concentrated toward the stellar equatorial plane. To distinguish between these options we next consider photometric and polarimetric variability.

7. Correlation of accretion with large amplitude photometric variability

7.1. *Stars with large amplitude photometric variability*

Bibo & Thé (1991) have noted that approximately 27% of the Finkenzeller & Mundt (1984) sample of HAeBe stars were large amplitude ($\geq$ 1 magnitude at V), irregular light variables. Nine of our program stars with accretion signatures were included in the study of Bibo & Thé (1991). Eighteen of the program stars are listed in the compilation of Schevchenko et al. (1994). All of the stars in common with our program which show photometric variability larger than 1 magnitude are stars with accreting gas detections in the optical or in our UV data. Inspection of the SIMBAD database for the other program stars shows that HD 45677, HD 37806, and HD 37062 are also large amplitude variables.

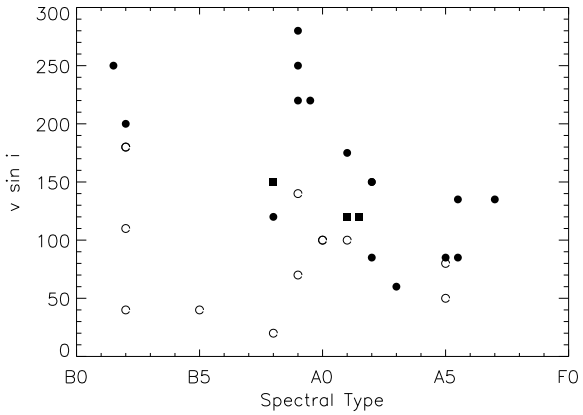

Fig. 21. Distribution of accretion and outflow signatures as a function of spectral type and v sin i. Open diamonds indicate the stars with spectral signatures of stellar winds. Filled circles indicate the stars with spectral signatures of accreting gas. Filled squares indicate the program stars with either winds or accreting gas

7.2. *Lack of a threshold for variability at A0*

Previous studies (Finkenzeller & Mundt 1984; Bibo & Thé 1991) have noted that large amplitude light variations were restricted to stars later than A0 in spectral type. Our data do not support the reality of such a limit, and suggest, instead, that it was the result of classification selection effects, since emission line B stars historically have been classified as Herbig Be stars only if they were located in extensive reflection nebulosity. We suspect that the number of stars in our survey with accreting gas with optical detections of large amplitude variability is a lower bound to the true number, since several of the program stars with accretion (HD 37411, HD 100546, HD 95881, HD 35929, HD 37806) have only recently been considered as HAeBe stars and lack an extensive history of photometric monitoring. Our detection of photometric variability in HD 95881 of 0.6 magnitudes ($V_{\rm FES}$) provides additional support for this interpretation. In contrast, the HAeBe stars with outflow signatures, many of which have been extensively monitored since the 1960s, typically have light variations below this level and usually below 0.25 magnitudes. Grinin et al. (1995b) have reached similar conclusions from a study of optical spectra and optical polarimetry and photometry.

8. Correlation of accretion with polarimetric variability

Grinin et al. (1991, 1994a,b, 1995a,b) have identified a population of comparatively isolated HAe stars with large amplitude light variations which are inversely correlated with broad-band linear polarization changes. For these stars, at optical minimum, the V-band linear polarization typically reaches 6−8%, values typical of more heavily obscured pre-Main Sequence (PMS) objects. For all of these stars the wavelength dependence of the polarization is consistent with scattering by dust in a flattened axisymmetric structure which is most probably a disk. Appreciable values of linear polarization comparable to the minimum light polarization values in Monte-Carlo simulation of dust envelopes around such stars are achieved only for orientations placing the line of sight to the star close to the disk plane (Voshchinnikov & Karjukin 1994; Voshchinnikov et al. 1995). The polarization data are most sensitive to the presence of dust in the immediate vicinity of the star and are comparatively insensitive to more distant material. Four of the stars considered in this study, UX Ori, BF Ori, RR Tau, WW Vul, as well as the early-type T Tauri stars CQ Tau (F2e) and BM And (G8e) have been studied by Grinin and collaborators and all show accreting gas in their optical spectra, and in the case of UX Ori in the LWP spectrum reported by Grady et al. (1995). The presence of similar polarimetric variations in HD 45677 (Schulte-Ladbeck et al. 1992) , VV Ser (Khardopolov et al. 1991), and HR 5999 (Hutchinson et al. 1994) all of which show accreting material in their UV or optical spectra, strongly imply that the accreting gas and the circumstellar dust have the same spatial distribution with respect to the star, as would be expected if the accreting, atomic gas is produced by disruption of circumstellar dust grains.

9. Geometry of the accreting material

The detection of polarimetric variability, large amplitude light variations, accreting gas, in stars with $v \sin i$ data suggesting that we view the star close to equator-on imply that the bulk of the circumstellar material is confined to a flattened, disk-like geometry with mid-plane probably coincident with the stellar equatorial plane. The indirect signatures of system geometry available to us do not permit us to distinguish between lines of sight which are truly equator-on and those which graze the outer, optically thin portions of a more vertically extended disk. However, the absence of polarimetric and light variations in the bulk of the stars with stellar wind detections does not support the suggestion of Herbst et al. (1994) that the bulk of the optical minima are caused by obscuration by dust clouds at high latitude with respect to the disk (e.g. dust clouds in a bipolar flow or in the line of sight when the star is viewed close to pole-on). In particular, such a geometry would not produce the large minimum light polarization values which are routinely observed in HAeBe stars (Grinin et al. 1991; 1992; 1994; 1995).

9.1. *Comparison with classical T Tauri stars*

This is in contrast to lower mass PMS stars, such as the classical T Tauri stars (Edwards et al. 1994) for which accretion and outflow signatures are routinely observed in the same spectrum, and accretion is detected in stars for which rotation period data combined with $v \sin i$ measurements imply that the star is viewed at low inclination. The lack of accretion signatures at high polar latitudes in our HAeBe stars suggests that accretion mechanisms involving magnetic channelling of material from the disk plane to high latitudes on the star (Shu et al. 1994a,b; Ostriker & Shu 1995) are probably not effective toward the end of the PMS lifetimes of intermediate-mass stars. Our data do not permit us to assess whether such magnetically channelled accretion is important earlier in the lifetime of intermediate-mass stars.

9.2. *Support for cleared regions surrounding the HAeBe stars*

The presence of accreting material with free-fall velocities in the line of sight of the disk further implies that, deep in the gravity well of the star, the density of circumstellar material drops sufficiently low that viscosity is unimportant in slowing the accreting gas to values expected for a classical accretion disk, or the inner disk of a classical T Tauri star. Similar density decreases for the HAeBe stars with IR spectral energy distributions which can be fit as 2 components have been inferred by Bogaert et al. (1995), and support interpretation of the IR excesses of these stars as indicating the presence of substantially cleared inner disks (Hillenbrand et al. 1992). One possible mechanism for clearing the inner part of a pre-existing Keplerian disk left over from star formation could be provided (if the star is rotating) by entrainment of disk material by a stellar wind, via the wind-induced accretion mechanism (J.E. Bjorkman & Wood 1995). Recent model calculations of accretion from a flattened circumstellar envelope rather than a spherical one (Calvet 1995) predict that accretion should occur preferentially in the plane of the dust disk, in agreement with our observations.

10. Comparison with β Pic

10.1. *Spectral similarity to β Pic*

The UV high dispersion data for HAeBe stars, together with the photometric and polarimetric variability data, imply that spectroscopic signatures of accreting, circumstellar gas are routinely observed for the less heavily obscured PMS A and B stars whenever the star is viewed close to equator-on, with the line of sight transiting the

circumstellar dust disk. This is essentially the same geometry inferred for the nearby β Pic disk. Our data suggest that the velocity range over which the accreting gas is observed does not change significantly from inferred system ages of 2−3 Myr (e.g. UX Ori) to at least the ZAMS (β Pic; Lanz et al. 1995) or beyond. In all cases the inferred velocities are consistent with material in free-fall toward the star (Walker 1972).

Spectroscopically, the accreting gas profiles seen in our program stars are similar to those seen toward β Pic, with the exception of apparent column densities which are a factor of at least 100−300 times higher. Local enhancements in the apparent column density are observed toward many of our program stars and are especially prominent in the 50−150 km s^{-1} range. Striking variability in this high velocity gas is seen in HD 45677, HD 50138, HD 100546, and HR 5999. Where optical monitoring data are available (de Winter 1996), the high velocity portions of the accreting gas profile are the most variable and clearly show large night-to-night changes. The available data therefore suggest that the accretional activity seen toward β Pic (Vidal-Madjar et al. 1994 and references therein) began during the earlier PMS evolution of the star and its circumstellar disk.

The presence of similar, high velocity, accreting gas toward three stars without net Hα emission, HD 37062, HD 176386, and V372 Ori, as well as the more recently studied V351 Ori (HD 38238, van den Ancker et al. 1995), all of which are near ZAMS or younger stars, strengthens the interpretation of β Pic as a comparatively young object (Lanz et al. 1995). The fact that β Pic has a larger IR excess, particularly at shorter wavelengths, corresponding to dust located closer to the star, than other field A shell stars with signatures of accreting gas (Grady et al. 1995b), supports interpretation of the large, and IR-bright β Pic disk as a comparatively short-lived, but normal phase in the evolution of A-star dust disks rather than as a unique or pathological object.

The association of accreting gas with polarimetric signatures of a disk system viewed close to equator-on suggests that spectroscopic surveys, complemented by polarimetric and photometric data, may provide an efficient means of identifying circumstellar disk systems oriented like β Pic.

10.2. *A possible mechanism: Accreting planetesimals*

The most extensive interpretation of the variable accretion seen toward β Pic models the gas features as comae of "infalling, evaporating bodies" with compositions assumed to be like that of Solar System comets on high eccentricity orbits similar to those inferred for Sun-grazing comets and bodies like Shoemaker-Levy 9 (Beust et al. 1993; Beust & Lissauer 1995). The association of the spectral features in the β Pic system with infalling solid bodies is indirect since *accreting* molecular and/or atomic gas, the expected precursors of the ionic species which are observed infalling toward the star, have not been seen.

The available data suggest that the link between the spectral signatures of gaseous accretion and solid bodies may be much less indirect for the HAeBe stars. Two of the HAeBe stars with accreting gas are known to be mid-IR photometric variables (Sitko et al. 1994; Hutchinson et al. 1994), with increasing IR excess consistent with production of warm dust observed in association with optical minima. Such variability is consistent with a high eccentricity body having a star-grazing encounter with enhanced dust production close to periastron passage. The observed brightness increase in the light curves of a number of the large amplitude photometrically variable HAeBe stars noted by Herbst et al. (1994) may be due to increased reflection of starlight from the stellar hemispheres not directly visible to us due to an increase in near-stellar dust immediately following optical minimum.

As noted by Grinin et al. (1994), the high velocity atomic gas observed in Na I and, in a number of our program stars, in C I and Mg I, implies in situ production of the gas from grain destruction, with the grains originally part of a larger parent body. The simplest mechanism for producing large numbers of small grains with velocities in excess of 100 km s^{-1} is by evaporation of a larger solid body with this bulk velocity (e.g. something like a comet), since alternate mechanisms (e.g. Poynting-Robertson drag) produce low velocity bulk motions only. This suggests that many of the spectral features of accretion that we observe are signatures of "secondary" accretion from accretion of planetesimals, rather than primary detections of accreting gas which is transported toward the star in an accretion disk. In tandem with the β Pic data, our detections of accretion imply that clumpy or "secondary" accretion becomes detectable while the star is still comparatively young. Recent studies of A-shell stars (Grady et al. 1996) suggest that such accretion may continue during much of the main sequence lifetime of the star, a period comparable with the epoch of high bombardment in the terrestrial planet region of our own Solar System.

10.3. *Implications*

Recent studies of the β Pic system have suggested that the high number of spectral accretion "events" can only be produced if there are large (e.g. gas giant masses) bodies in the system which can perturb smaller planetesimals into the requisite high eccentricity orbits via secular or mean motion resonances. If these mechanisms are applicable to our younger HAeBe stars, the spectral data provided by the IUE and ESO observations imply not only that bodies resembling our expectations for planetesimals are present in these systems at ages of a few Myr, but also that larger planets may have formed. Recent studies of planet formation have indicated that terrestrial-mass planetary cores

can be easily produced in minimum mass solar nebula disks in 10^{5-6} years, and that additional runaway processes can result in the accretion of the gaseous envelopes in a few million years (Lissauer 1995), values consistent both with statistical studies of the dissipation/accretion of circumstellar dust disks (Strom et al. 1993) and with the PMS evolutionary lifetimes of intermediate-mass stars (Palla & Stahler 1993). If correct, the prospects for planet search programs, beyond those focussing on radial velocity variations of nearby, late-type stars, such as are being considered as part of the NASA Exploration of Neighboring Planetary Systems program, are promising. The HAeBe star data will further constrain models for the β Pic system: any mechanisms, such as secular or mean motion resonances, capable of accounting for the falling evaporating bodies in the β Pic system must be sufficiently general to produce similar activity in the disk of essentially any suitably oriented PMS A star.

Acknowledgements. We wish to thank Lynne Hillenbrand, Louma Ghandour, and Steve Strom for pre-publication release of their v sin i data for a number of the HAeBe stars discussed in this paper. We also wish to thank both Lynne Hillenbrand and Nuria Calvet for a critical reading of this paper while still in manuscript form. Support for this study was provided by the Long-Term Space Astrophysics Program under NASA contract NASW 4756 to the Applied Research Corporation and to Eureka Scientific. IUE Observing time used in this program was provided by NASA programs ASRKB, PPPCG, PPQCG, and VILSPA program RM048. Support for observational research at Ritter Observatory is provided by The University of Toledo and NSF grant AST-9024802 to B.W. Bopp. Technical support is provided by R.J. Burmeister and C.L. Mulliss. MB's participation in this research is supported by the Research Experiences for Undergraduates program of the National Science Foundation. Computing resources for the analysis of the IUE data were provided by the IUE Data Analysis Center located in the Laboratory for Astronomy and Solar Physics of NASA/GSFC. IRAF is distributed by the National Optical Astronomy Observatories, which are operated by the Association of Universities for Research in Astronomy, Inc., under contract with the National Science Foundation. This study has made use of the SIMBAD database, operated at CDS, Strasbourg, France.

Table 4. Log of the Optical spectroscopic observations. ESO spectra were obtainedin two wavelength regions entered on Hα, 6536−6591 Å(R=50 000), andthe Na I D and He I 5876 Å lines (R=55 000), 5861−5917 Å. Ritter Observations provide simultaneous observation of both Na I D and Hα with R=25 000. The CTIO spectra were obtained with the 1-m telescope and 2D-Frutti with $R\sim$1300. The first column lists the star. The second column gives the spectral segment covered. The third column gives the date of observation as JD-2440000. The fourth column identifies the observing site with E=ESO, R=Ritter, C=CTIO. The remaining columns give the exposure duration in minutes, the resolving power of the spectra and the continuum S/N

Object	Line	JD	Site	Exp.	S/N
HD 37806	Na I, Hα	9801.5468	R	60	40
HD 50138	Na I, Hα	9705.7014	R	60	140
HD 100546	Hα	9184.576	E	15	200
	Na I	9187.501	E	15	173
HD 58647	Hα	9732.2898	E	20	182
	Na I	9733.3016	E	15	125
NX Pup	Hα	9732.3154	E	45	20
	Na I	9733.3251	E	45	50
UX Ori	Hα	9272.8479	E	30	42
	Na I	9272.7188	E	50	50
HD 95881	Hα	9732.3617	E	40	13
	Na I	9733.3685	E	45	125
HD 35187	Na I, Hα	9410.5534	R	60	40
VV Ser	Hα	9187.605	E	60	14.1
V586 Ori	Hα	9736.0831	E	45	56
	Na I	9736.2348	E	45	50
HK Ori	Hα	9733.0854	E	45	12
	Na I	9735.0841	E	45	25
KK Oph	Hα	9184.697	E	60	25
	Na I	9185.688	E	60	2.0
BF Ori	Hα	9269.8931	E	27	13
	Na I	9272.7820	E	60	17
	blue	9365	C		
HR 5999	Hα	9184.624	E	15	200
	Na I	9185.656	E	20	500
T Ori	Hα	9736.1574	E	45	63
	Na I	9736.1979	E	45	50
V346 Ori	Hα	9735.1305	E	45	29
	Na I	9735.0477	E	45	42
HD 35929	Hα	9363.614	E	30	60.7
	blue	9365	C	20	

A. Individual stars with accreting gas

Individual program stars with accreting gas are discussed below. The journal of optical observations is given in Table 4.

A.1. *HBe stars with IUE high dispersion spectra*

HD 37062 (B1.5): - While SIMBAD lists a spectral type for this star of B5 V, comparison of the FUV spectrum, particularly the region near Si III (4) and Si II (2), suggests a spectral type of B1.5, and certainly not later than B2. Comparison with IUE spectra of rapidly rotating Be stars from the catalog of Slettebak (1982), which provides the densest grid of uniformly measured v sin i for rapidly rotating early B stars, suggests that v sin i for HD 37062 is at least 250 km s^{-1}. IUE spectra for this star were obtained on 3 dates in 1982-1984. In the 1981 April spectrum, C IV shows flat absorption troughs out to +200 km s^{-1} some 22% above zero flux in both members of the resonance doublet, implying optically thick absorption with ≈78% covering factor. There is a hint of some weak emission extending at most 10% above the local continuum on the short wavelength wing of the absorption, which is not seen in the later spectra. The Si IV absorption resembles C IV.

HD 45677 (B2[e]): The presence of high velocity, accreting gas was reported by Grady et al. (1993a), following up on the detection of a UV-optical polarization position angle rotation (Schulte-Ladbeck et al. 1992). FUV spectra, and the implications for the grain characteristics in the circumstellar disk, are discussed by Brown et al. (1995). Sitko et al. (1994) and van den Ancker et al. (1996) have summarized the history of UV and optical light variations in this object. Spectra and optical photometry obtained in 1994 December indicated V=7.9, e.g. only 0.35 magnitudes below the historical optical maximum of 7.55. The mid-UV spectrum at this light level is close to losing any detectable Fe II emission. In the FUV the spectrum shows enhanced outflow signatures in Si II, Al II, Al III, Fe III and similar ions, with accretion still visible to +400 km s^{-1} in C IV and Si IV. Recently, Israelian et al. (1996) have suggested, on the basis of optical He I profiles, that v sin i=70 km s^{-1} for this star. Comparison of UV spectra in the range 1500−1600 and 1800−1900 Åwith B2 stars with v sin i measurements from Slettebak (1982) show that the UV spectrum of this star is heavily veiled compared to stars with v sin $i \leq$ 160 km s^{-1}, suggesting that either the star has a higher v sin i or that the UV continuum is sufficiently veiled that the stellar photosphere is not seen. We therefore favor a v sin i closer to the 200 km s^{-1} of Swings (1973).

HD 37806 (B8e): High dispersion FUV spectra of this star have been obtained on 3 occasions with no indication of significant continuum variability. The mid-UV spectrum shows a type I P Cygni profile in Mg II (1) with peak emission some 2× the local continuum level. The absorption shortward of the emission is centered at +10 km s^{-1}, with peak absorption coincident in velocity with essentially saturated Mg I absorption. Mg II (3) is detected in a feature centered at +110 km s^{-1}. Accreting gas is detectable in the FUV data, especially in Al III (1) and Fe III (34). The Fe III absorption shows a flat absorption trough over −25 to +125 km s^{-1} with a covering factor of 65%. The red wing of this profile can be followed to +250 km s^{-1}. Al III (1) is similar with a slightly higher covering factor, excess absorption visible on the shortwavelength wing of the profile to −140 km s^{-1} and absorption on the red wing of the profile visible to at least +350−400 km s^{-1}. C IV is represented by saturated absorption in both members of the resonance doublet with a weak blue wing to −225 and absorption on the red wing which can be followed to +400 km/s. Si II (2) shows saturated absorption in the transition to the excited J-level at 1533.4 Å , with absorption on the red wing of the line profile which can be followed to +200 km s^{-1}. Al II is similar. C I absorption is visible without obvious variability or extremely high velocity extension in multiplets 2, 3, and 4. Given the large range of oscillator strengths involved, detection of all three multiplets demonstrates a circumstellar origin for this atomic gas and also the Mg I seen in the mid-UV data. In our optical spectrum, He Iλ 5876 is a symmetrical absorption feature centered at a heliocentric radial velocity of +45 km s^{-1}. Na I is weakly in emission and Hα shows a type III P Cygni profile.

HD 50138 (B8[e]): The presence of redshifted absorption features was first reported by Hutsemékers (1985), and has more recently been studied by Morrison & Beaver (1995) who found inverse P Cygni type I profiles in Si II and He I. The similarity to other Herbig Be stars was noted by Grady et al. (1993). Mg II in this object, which has been monitored sporadically by the IUE from 1979 through 1995, alternates between classical type I P Cygni emission and type III emission. The $V_{\rm FES}$ data for this star suggsests that 6.5$\leq V \leq$6.8 for all of the IUE observations. Weak emission is present in the Fe II multiplets visible in the IUE mid-UV data. Mg I absorption is visible with absorption on the red wing which can be followed to +80 km s^{-1} and is variable. C I is present, but is heavily contaminated by absorption from nearby Fe II lines, precluding analysis. Si II in this star shows saturated absorption from −100 to +50 km s^{-1} with a strong red wing visible to 250−300 km s^{-1} in the recent spectra. Al II is similar to Si II in this star. Al III and Fe III (34) show prominent absorption beginning slightly blueward of the transition rest wavelength and visible to +425 and 300 km s^{-1}, respectively. C IV in all spectra shows accreting gas visible to +400 km s^{-1}. The profiles are typically flat absorption troughs over the initial 150−200 km s^{-1} with a covering factor of approximately 60%. Weak emission up to 10−15% of the local continuum level is present in some of the spectra, and is clearly variable. Polarimetric observations for this star are presented by Bjorkman & Schulte-Ladbeck (1994), and in Vaidya & Schulte-Ladbeck (1995).

HD 100546 (B9e): The IR spectral energy distribution for this star was first discussed by Hu et al. (1989). Bogaert et al. (1995) show the IR spectral energy distribution in more detail, together with the prominent dip near 10 μm. Henning et al. (1995) infer a disk extent, from modelling of the IR and sub-mm emission, of 660 AU. IUE high dispersion spectra have been obtained on 5 dates with $V_{\rm FES}$ near 8.2 and with the bulk of the FUV and mid-UV data non-simultaneous. The presence of redshifted Lyα emission was noted by Talavera et al. (1994). The majority of C IV profiles for this star, however, show inverse type I P Cygni emission, with the emission as much as 20−25% above the local continuum and absorption extending to 400 km s^{-1}. Si II (2) and Al II (2) shows hints of similar, although weaker emission and absorption. In the earlier spectra, circumstellar Fe II emission, while clearly present, cannot be followed to velocities higher than +100 km s^{-1}. Mg II shows inverse type I P Cygni emission similar to the C IV profile. Intercomparison of the archival data and spectra obtained in 1995 March shows striking variability in the high velocity portions of the Mg II, Fe

II, Si II, Al II, C IV, Si IV, and C I profiles (Fig. 18). C I absorption can be followed in the 1995 data to +200 km s^{-1} relative to the star. Mg I absorption, while detected at low velocity, shows no obvious variability. ESO CAT observations from July 18, 1993 show a type III P Cygni profile in Ha with $V \geq R$. Na I is present, and comparatively weak, suggesting a foreground IS origin. He I λ 5876 is present in absorption.

HD 58647 (B9): IR data for this star are presented in Oudmaijer et al. (1992) and Bogaert et al. (1995). Thé et al. (1994) reported this star as a non-emission line star with optical shell spectrum. Optical spectra obtained in 1995 January at ESO reveal P Cygni type III emission in Hα, implying that this star is a bona-fide Herbig Be star. Na I on the same date showed sharp IS-like absorption and no He I absorption. IUE observations obtained on 1994 Dec. 12 show inverse type I P Cygni profiles in Mg II (1) superposed on the wings of photospheric Mg II absorption. Comparison with other B9e stars from the catalog of Slettebak (1982) suggests v sin i is near 280 km s^{-1}.

A.2. *HAe stars with IUE high dispersion spectra:*

NX Pup: HST FGS data for this star have indicated that the optically visible star consists of a HAe star with nearby (d=0.″12) lower-mass companion (Bernacca et al. 1993), with an additional Hα emission-line star located some 7″ from NX Pup A (Tessier et al. 1994). Additional Hα emitters are are visible in Fabry-Perot images centered at larger distances. The coarse spatial resolution of the IRAS SCANPI or even HIRES data includes, therefore, emission from NX Pup A, emission from what is clearly a T-association, and the nearer portions of CG 1 (Reipurth 1983), and thus overestimates the emission from NX Pup A. IUE low dispersion data show unusually strong Mg II emission for an early A spectral type in all observations. Our high dispersion spectrum from 1994 April shows prominent type III emission in Mg II, and detectable Mg I absorption at very low S/N. When compared with A1e-sh star spectra, weak emission is visible in the Fe II multiplets.

UX Ori (A1-IIIe): The presence of accreting gas in this prototype of the isolated HAe stars with large amplitude light variations and spectacular polarimetric variability is reported by Grinin et al. (1994b). Na I absorption profiles, complete with features similar to the discrete absorption components seen in β Pic, vary from night to night and are discussed by de Winter (1995). The single mid-UV high dispersion spectrum for this star is discussed by Grady et al. (1995a), together with the available low dispersion spectra.

HD 37411 (B9e): This star is represented in the IUE archives by a lone LWP high dispersion spectrum with S/N=7 near 2810 Å . The Mg II profile for this star is shown in Imhoff (1994) who noted trough-like absorption in both members of Mg II (1). Mg I absorption is essentially saturated and centered at +30 km s^{-1}. Strong transitions from Fe II (62,63) are present and centered at +50 km s^{-1} with wings visible to +80 km s^{-1}.

HD 95881 (A2e): The presence of a large IR excess consistent with circumstellar dust was noted from IRAS data by Oudmaijer et al. (1992) and subsequently characterized by Bogaert et al. (1995). Low dispersion IUE spectra show a spectrum consistent with an early A spectral type, but with strong Fe II line blanketing. Mg II appears filled in relative to the expected photospheric absorption at this resolution. High dispersion LWP spectra show, in the brighter of the 2 spectra, Mg I absorption which is saturated and centered at +10 km s^{-1}, with a FWHM=60 km s^{-1}. The FWHM of the Mg I is clearly variable. Mg II exhibits type I or III P Cygni emission, if no allowance is made for the expected strong, photospheric Mg II absorption at this spectral type. When compared to the A2-sh star HR 10 (HD 256, v sin i=195 km s^{-1}), HD 95881 clearly exhibits type III P Cygni emission in Mg II, with, however some modification of the profile by additional absorption features. In our data $R \geq V$ in Mg II. Fe II in this star shows prominent low velocity absorption in transitions to the ground configuration over −20 to +60 km s^{-1}, as well as a strong, broad absorption component centered at roughly +70 km s^{-1} in the brighter of the 2 spectra. Circumstellar absorption can be followed to +250 km s^{-1} in Fe II. The high velocity feature is greatly diminished in the 1995 May 25 spectrum. Mg II (3) at 2790.3 Å is entirely redshifted, with absorption peaking at +70 km s^{-1} and absorption extending to 200 km s^{-1}.

HD 35187 (A2e): A large IR excess due to circumstellar dust was initially noted by Walker & Wolstencroft (1988) with more recent data in in Bogaert et al. (1995). Prominent photospheric absorption consistent with the early A spectral type is visible in the wings of Mg II (1) with, however superposed absorption in 3 components visible at +40, +80, and +130 km s^{-1}. When compared with the A1e-sh star HD 15253, some filling in of the Mg II profile on the blue wing is apparent, suggesting that we may have an incipient inverse P Cygni profile in this star. Mg I shows a single absorption component at +40 km s^{-1} with a strong red wing visible to +80 km s^{-1}. Fe II (1) absorption is present over essentially the same velocity range as the Mg II features. Weak Fe II (62,63) absorption is present coincident with the lower velocity Mg II features, demonstrating a circumstellar origin for the features. Hα shows a type III P Cygni profile, with, however, asymmetric absorption resembling that seen in UX Ori extending to +100 km s^{-1}. Na I is consistent with photospheric and foreground IS absorption.

HR 5999 (A5-7IVe) This HAe star located in Lupus T3 at a distance of 140 pc (Hughes & Hartigan 1993) has a history of large amplitude photometric variability (Bibo & Thé 1991) with polarimetric variability

discussed by Hutchinson et al. (1994). The presence of high velocity, accreting circumstellar gas was reported by Pérez et al. (1993). Redshifted Lyman α emission was reported in deep FUV high dispersion spectra obtained at optical maximum light by Blondel et al. (1994). Lyman α shows emission throughout the photometric range of this star in IUE low dispersion spectra (Pérez et al. 1993b). Circumstellar extinction for this star is discussed in Thé et al. (1995).

HD 35929 (A8e): IR data for this star are given in Oudmaijer et al. (1992) and discussed in more detail in Bogaert et al. (1995). IUE low dispersion observations of this star are consistent with a spectral type of A8-F0, but not later than F2 with $E(B-V)$=0.10−10.12, of which 0.06 is plausibly due to the ISM. The IUE fluxes lie systematically below the TD1 measurements, suggesting that this object may be a photometric variable. IUE mid-UV spectra obtained in 1994 January and 1995 March both show type III P Cygni emission in Mg II (1), superposed on broad, photospheric absorption wings. Comparison with the A7 IV-sh star HD 98080 (Slettebak 1992) suggests that $v \sin i$ for this star is between 150 and 200 km s^{-1}. Fe II absorption is present, but is detectable only at low S/N. Our 1994 March FUV high dispersion spectrum shows Zn II absorption visible to +110 km s^{-1}. Deep low dispersion spectra obtained in 1994 January and 1995 March show prominent C IV and O I emission, similar to that seen toward other late HAe stars (Pérez et al. 1993). ESO CAT and Ritter Observatory echelle spectra from 1994 January show a single emission peak at Hα with excess emission on the red wing superposed on the wings of photospheric Hα absorption. The Na I profile is consistent with photospheric absorption and a foreground IS feature. Our CTIO low resolution spectrum from 1994 January 12 shows the Balmer series clearly present in absorption from Hβ through Hι. Absorption features at 3933 and 3970 Å are tentatively attributed to Ca II K and H, respectively. Some contamination due to He is likely in the 3970 Å feature since it is stronger than either of the adjacent Balmer lines. Ca II K 3933 Åhas W_λ=4.6±1 Å .

A.3. *Stars with optical detections of accretion only:*

R CrA (B8e): The presence of high velocity, accreting gas was reported by Graham (1992). The IUE low dispersion data, obtained at V=12.7, show a FUV spectrum consistent with a spectral type no later than late B. Na I in the star is routinely observed in emission. Hamann & Persson (1992) show O I inverse P Cygni profiles for this star, together with prominent, single emission features in Ca II.

RR Tau (A2e): The presence of high velocity Na I absorption with discrete absorption components and redshifted He I features was noted by Grinin et al. (1995). Hα in this star typically exhibits a type III P Cgyni profile. The data from Finkenzeller & Mundt (1984) show type III P Cygni emission in Hα and no detectable absorption in Na I. Strong Fe II and Mg II emission have been detected in the IUE spectra obtained at V=11.2.

VV Ser (A2e): Chavarría-K. et al. (1988) show type III P Cygni emission in Hα. Na I toward this star is characterized in their data, and in our ESO spectra, by narrow absorption features which are close to saturation. The Hα profile shown in Finkenzeller & Mundt (1984) shows a prominent wing on the red side of the central reversal in this transition. Na I data from the same epoch shows enhanced absorption visible to +150−200 km s^{-1}. He I shows redshifted absorption in the same spectrum. Hamann & Persson (1992) note the presence of weak blue-shifted emission in the O I λ 7773 triplet suggestive of inverse P Cygni profiles.

HK Ori (A3-4e): ESO spectra at Na I from 1993 October 12-13 show saturated low velocity Na I absorption with asymmetric absorption on the red wing of the profile which can be followed to slightly more than +100 km s^{-1}. IUE low dispersion spectra at V=11.9 show Mg II emission, together with truly spectacular emission from Fe II in both the mid and FUV. Data from Finkenzeller & Mundt (1984) shows type III P Cygni emission in Hα and Na I absorption characterized by a sharp absorption feature at low velocity, with enhanced absorption visible to between 150 and 200 km s^{-1}.

KK Oph (A5e): The presence of accreting gas was noted by Hamann & Persson (1992). Our ESO spectra show type III P Cygni emission in Hα, together with spectacularly variable emission on the red wing of the red emission profile. Na I shows high velocity accreting gas which can be followed to +150−200 km s^{-1}. Similar, but much stronger high velocity absorption is shown in Fig. 2 of Hamann & Persson (1992). Ca II λ 3933 and the IR triplet in their data shows unambiguously inverse P Cygni emission. Mg II and Fe II emission are detectable in IUE low dispersion spectra obtained at $V_{\rm FES}$=11.95.

BF Ori (A5e): The presence of accreting, circumstellar gas was reported by Welty et al. (1992). Monitoring of this star has revealed prominent, high velocity Na I absorption with discrete absorption components which vary from night to night (de Winter 1995). One mid-UV high dispersion spectrum of BF Ori showing emission at Mg II was obtained some 0.8 magnitudes below optical

maximum at $V_{\rm FES}$=10.5, but with a very low S/N. Fe II and Mg II emission are routinely observed near optical minimum light in this object.

T Ori (A5e): The presence of accreting gas was first noted at Hβ by Ghandour et al. (1994). Our Na I data shows redshifted Na I absorption to ≈+200 km s^{-1} with an absorption component at +100 km s^{-1}. Van den Ancker et al. (1995b) discuss the optical light variability in this star.

References

Aumann H.H., 1985, ApJ 278, L23
Beals C.S., 1950, Pub. Dom. Astr. Obs 9, 1
Bernacca P.L., et al., 1993, A&A 278, L47
Beust H., Lissauer J., 1995, A&A 282, 804
Beust H., et al., 1992, A&A 247, 505
Beust H., et al., 1994, ApSS 212, 147
Bibo E.A., Thé P.-S., 1991, A&AS 89, 319
Bjorkman J.E., Wood K., 1995, ApJ (submitted)
Bjorkman K.S., Schulte-Ladbeck R.E., 1994, ASP Conf. Ser. 62, 74
Blondel P.F.C., et al., 1993, A&A 268, 624
Böhm T., Catala C., 1994, A&A 290, 167
Bogaert E., et al., 1995, A&A (in press)
Boggess A., et al., 1991, ApJ 377, L49
Brown T.A., et al., 1995, ApJ 440, 865
Bruhweiler F.C., et al., 1989, ApJ 340, 1038
Calvet N., 1995, Revista Mexicana de A&A, Ser. Conf. 1, 193
Catala C., et al., 1991, A&A 244, 166
Chavarría-K. C., et al., 1988, A&A 197, 151
Davis R., et al., 1983, AJ 88, 1644
de Winter D., 1996, PhD Thesis, University of Amsterdam
Finkenzeller U., Mundt R., 1984 A&AS 55, 109
Finkenzeller U., 1985, A&A 151, 340
Edwards S., et al., 1994, AJ 108, 1056
Ghandour L., et al., 1994, ASP Conf. Ser. 62, 223
Grady C.A., et al., 1987, ApJ 320, 376
Grady C.A., et al., 1988, ESA SP-281, Vol. 2, p. 109
Grady C.A., et al., 1989, ApJ 339, 403
Grady C.A., et al., 1991, ApJ 367, 296
Grady C.A., Silvis J.M.S., 1993, ApJ 402, L61
Grady C.A., et al., 1993a, ApJ 415, L39
Grady C.A., et al., 1993b, A&A 274, 847
Grady C.A., et al., 1994, ASP Conf. Ser. 62, 409
Grady C.A., et al., 1995, A&A 302, 472
Grady C.A., et al., 1996, ApJL (in press)
Graham J.R., 1992, PASP 104, 479
Graham J.R., 1994, ASP Conf. 62, 363
Grinin V.P., et al., 1991, ApSS 186, 283
Grinin V.P., et al., 1994a, ASP Conf. Ser. 62, 130
Grinin V.P., et al., 1994b, A&A 292, 165
Grinin V.P., et al., 1995, A&A (in press)
Hamann F., Persson S.E., 1992, ApJS 82, 285
Henning T., et al., 1994, A&A 291, 546
Herbst W., et al., 1994, AJ 108, 1906
Hillenbrand L.A., et al., 1992, ApJ 397, 613
Hillenbrand L.A., et al., 1995, (private communication)
Horne K., 1986, PASP 98, 609
Hu J.Y., et al., 1989, A&A 208, 213
Hughes J., et al., 1993, AJ 105, 571
Hutchinson M.G., et al., 1994, A&A 285, 883
Hutsemékers D., 1985, A&AS 60, 373
Imhoff C.L., 1994, ASP Conf. Ser. 62, 107
Israelian G., et al., 1996, A&A 311, 643
Khardopolov V.I., et al., 1991, Astr. Zh. 68, 565
Kondo Y., Bruhweiler F.C. 198
Lanz T., Heap S.R., Hubeny I., 1995, ApJ 447, L41
Lecavelier des Etangs A., et al., 1995, A&A 299, 557
Lissauer J.J., 1995, Icarus 114, 217
Lagrange-Henri A.M., et al., 1990, A&AS 85, 1089
Lagrange A.M., et al., 1995, A&A 296, 499
Marlborough J.M., Peters G.J., 1986, ApJS 62, 875
Marsh K.A., et al., 1995, ApJ 451, 777
Morrison N.D., Beaver M., 1995, BAAS 27, 825
Ostriker E., Shu F.H., 1995, ApJ 447, 813
Oudmaijer R., et al., 1992, A&AS 96, 625
Palla F., Stahler S.W., 1993, ApJ 418, 414
Paresce F., 1991, A&A 247, L25
Pérez M.R., et al., 1993, A&A 274, 381
Praderie F., et al., 1986, ApJ 303, 311
Reipurth B., 1983, A&A 117, 183
Schevchenko V.S., et al., 1994, ApSS 202, 121
Schulte-Ladbeck R.E., et al., 1992, ApJ 401, L108
Sitko M.L., et al., 1994, ApJ 432, 753
Stencel R.E., Backman D.E., 1991, ApJS 75, 905
Slettebak A., 1982, ApJS 50, 55
Sonneborn, et al., 1988, ApJ 325, 784
Stapelfeldt K.R., et al., 1995, ApJ 449, 888
Strom S.E, Edwards S., Skrutskie M.F., 1993, in Protostars and Planets III. In: Levy E.H. and Lunine J.I. (eds.). Tucson: University of Arizona, p. 837
Shu F., et al., 1994a, ApJ 429, 781
Shu F., et al., 1994b, ApJ 429, 797
Talavera A., et al., 1982, Proceedings of the Third European IUE Conference, ESA SP-176, p. 99
Talavera A., Verdugo E., 1994, ASP Conf. Ser. 62, 136
Talavera A., et al., 1994, ASP Conf. Ser. 62, 115
Tessier E., et al., 1994, The Messenger 78, 35
Thé P.-S., de Winter D., Pérez M.R., 1994, A&AS 104, 315
Vaidya A., Schulte-Ladbeck R.E., 1995, BAAS 27, 825
van den Ancker M.E., et al., 1995a, A&A (submitted)
van den Ancker M.E., Glinos G., Thé P.S., 1995, A&A (submitted)
van den Ancker M.E., et al., 1996, (in preparation)
Vidal-Madjar A., et al., 1994, A&A 290, 245
Voshchinnikov N.V., Karjukin V.V., 1994, A&A
Voshchinnikov N.V., Grinin V.P., Karjukin V.V., 1995, A&A 294, 547
Walker M.F., 1972, ApJ 175, 89
Walker H.J., Wolstencroft R.D., 1988, PASP 100, 1509
Waters L.B.F.M., et al., 1988, A&A 203, 348
Welty A.D., et al., 1992, AJ 103, 1673